Physics with Exotic Nuclei

Hans-Jürgen Wollersheim

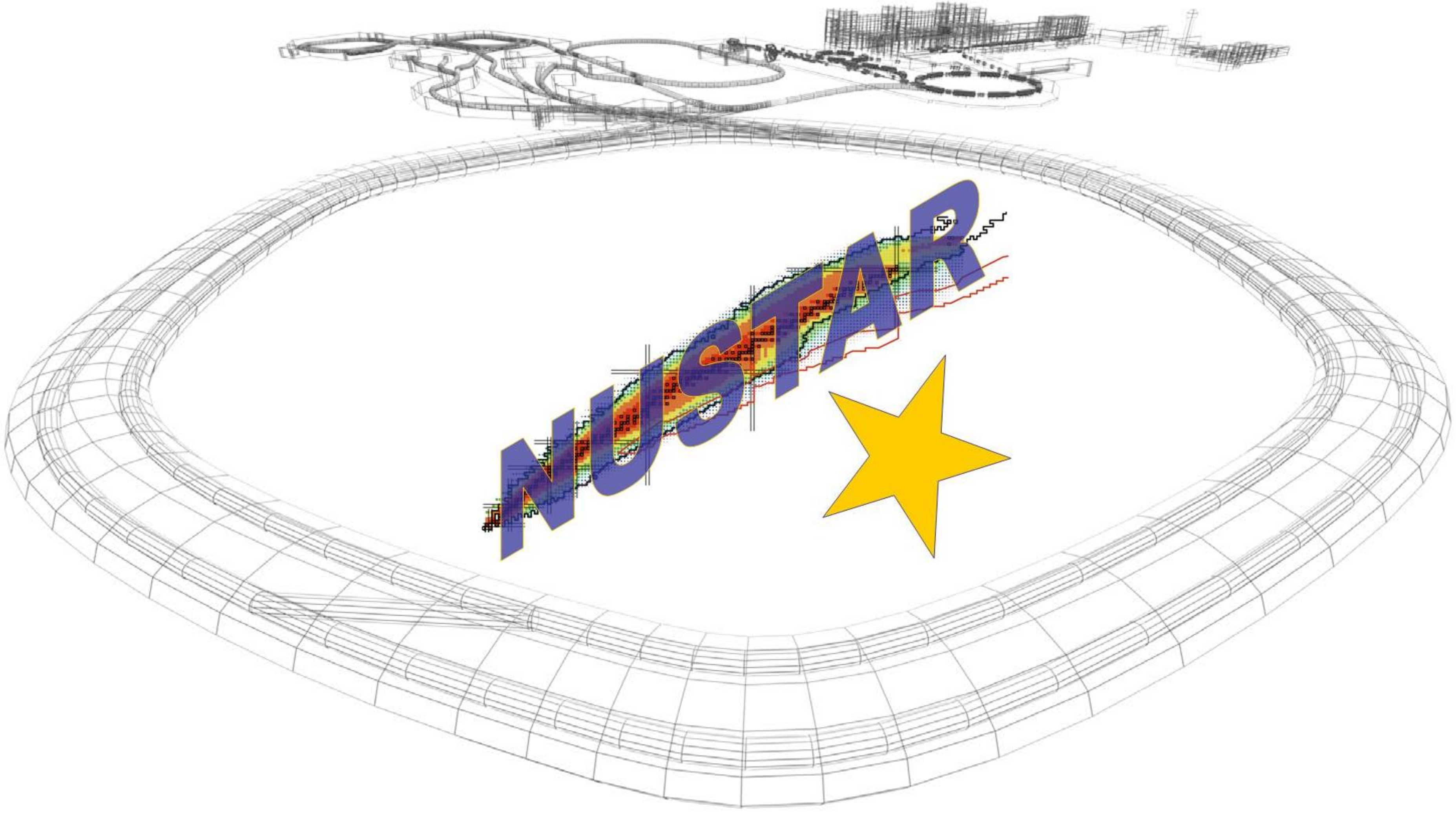

Outline

❖ **Scattering Experiments with RIBs – Nuclear Structure Results**

- Experimental evidence for closed-shell nuclei
- Scattering experiments at relativistic energies
- Projectile-like identification (Z, A) and scattering angle θ
- Doppler-shift correction of the emitted γ-rays

Physics with Exotic Nuclei

Experimental evidence for magic numbers close to stability

S. Raman et al., Atomic Data & Nuclear Data Tables 78, 1

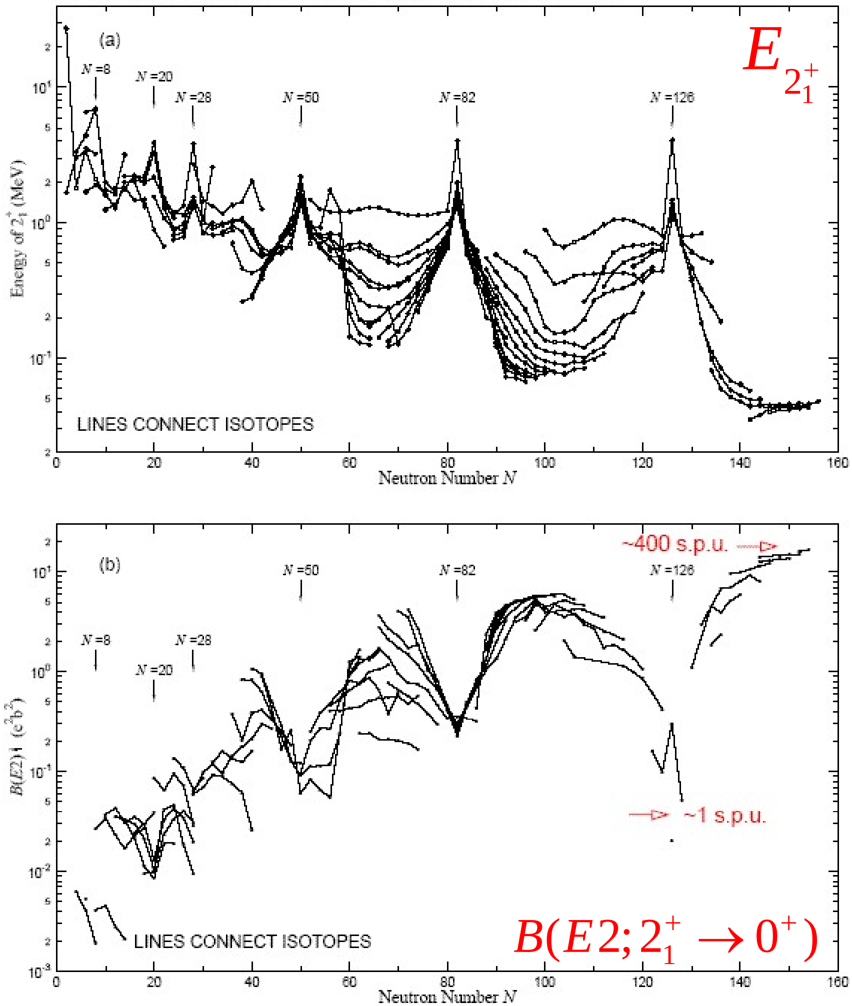

Table 1 -- Nuclear Shell Structure (from *Elementary Theory of Nuclear Shell Structure*, Maria Goeppert-Mayer & J. Hans D. Jensen, John Wiley & Sons, Inc., New York, 1955.)

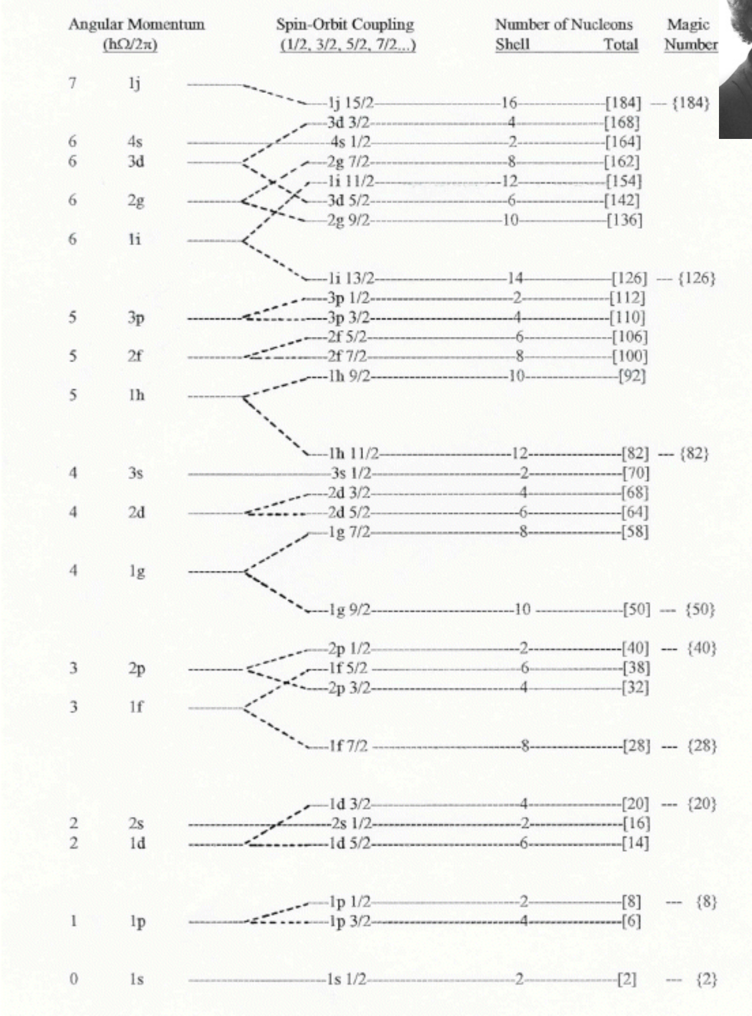

Physics with Exotic Nuclei

Experimental evidence for magic numbers close to stability

S. Raman et al., Atomic Data & Nuclear Data Tables 78, 1

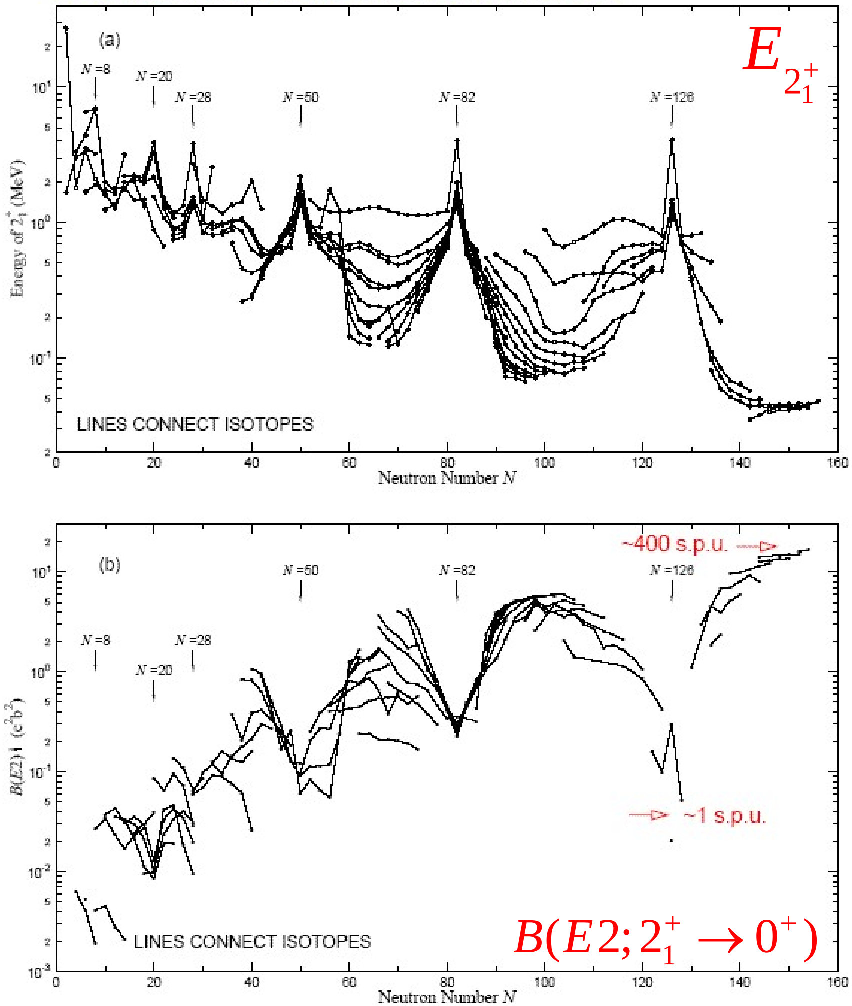

Nuclei with magic numbers of neutrons/protons

high energy of 2_1^+ state

low $B(E2; 2_1^+ \rightarrow 0^+)$ values

transition probability measured in single particle units (spu)

If we move away from stability?

Production, Separation, Identification

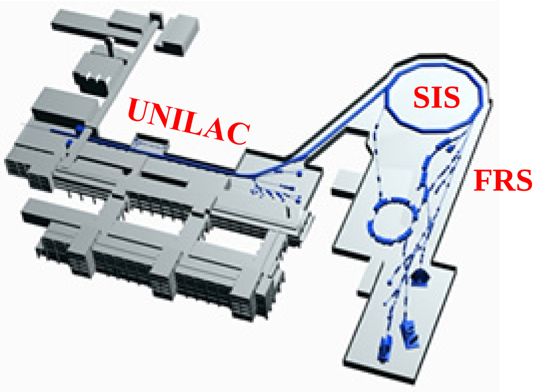

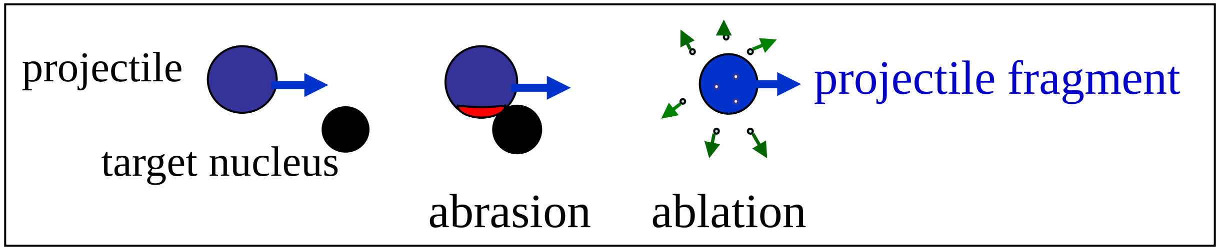

FRagment
Separator

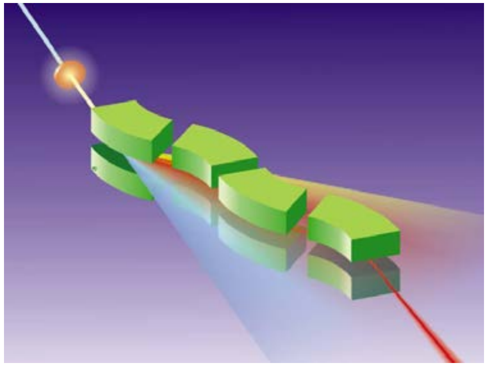

Standard FRS detectors

TPC-**x,y position**
@ S2,S4

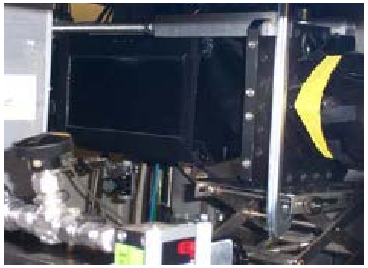

Plastic scintillator (**TOF**)
@ S4

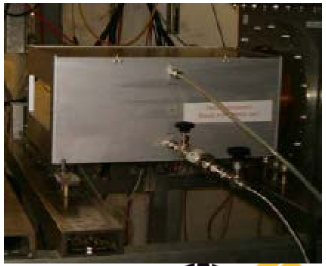

MUSIC (**ΔE**)
@ S4

Scattering Experiment at Relativistic Energies

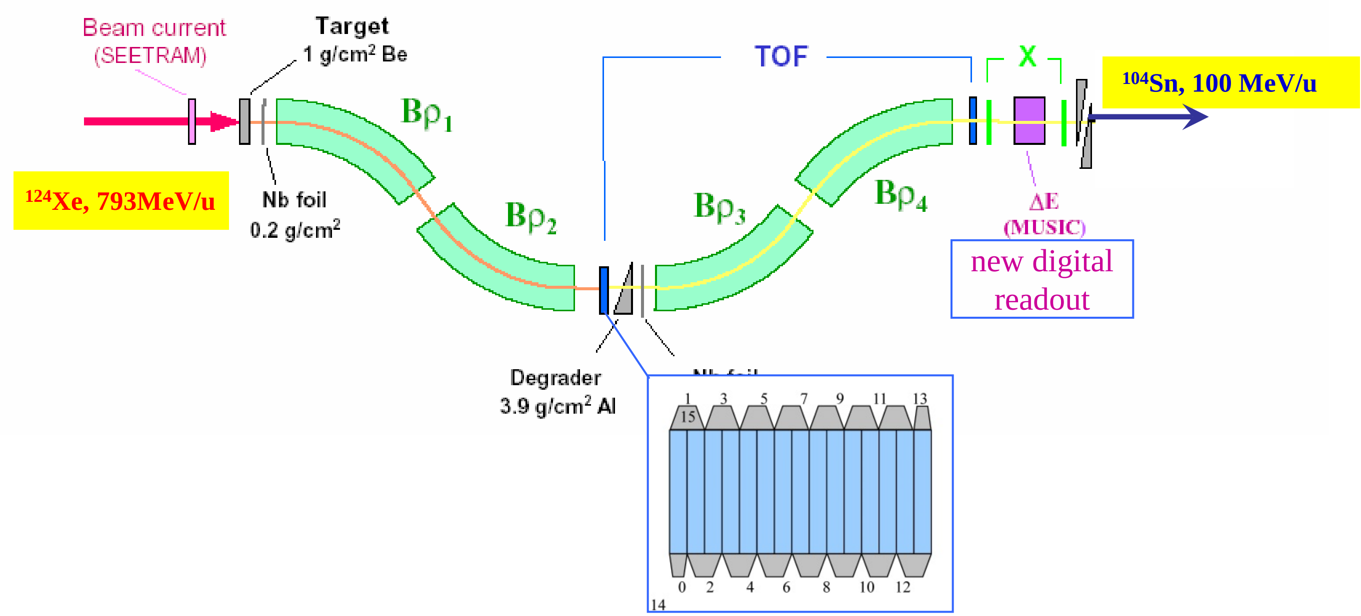

finger segmented detector

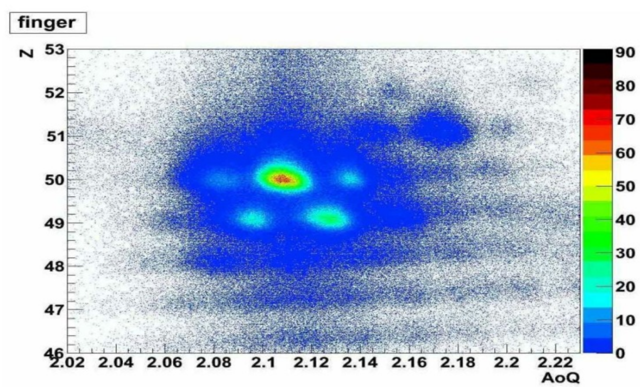

^{104}Sn fragments

using ^{124}Xe at 793 MeV/u

high rate at S2 ~10^{6} s^{-1}

- ~2400 % more tracking efficiency
- good A/Q resolving power

Scattering Experiment at Relativistic Energies

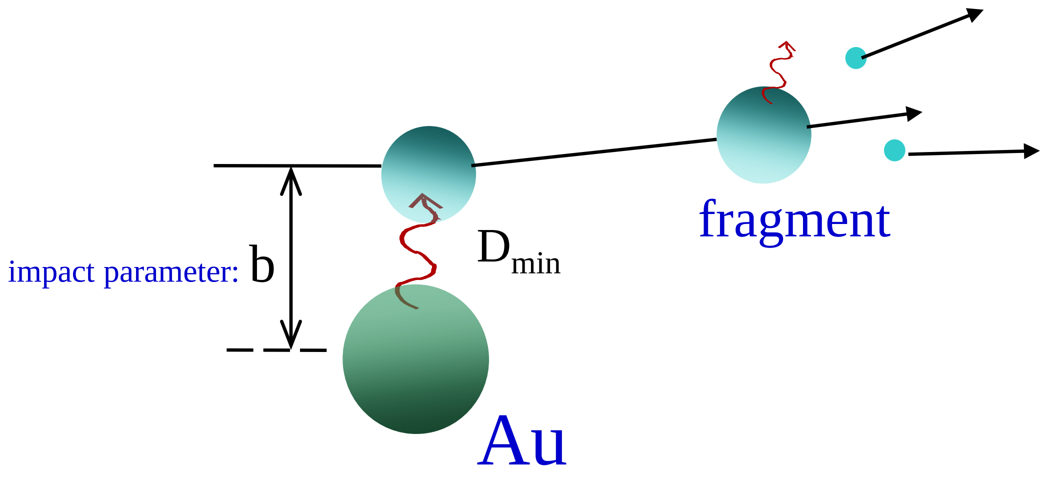

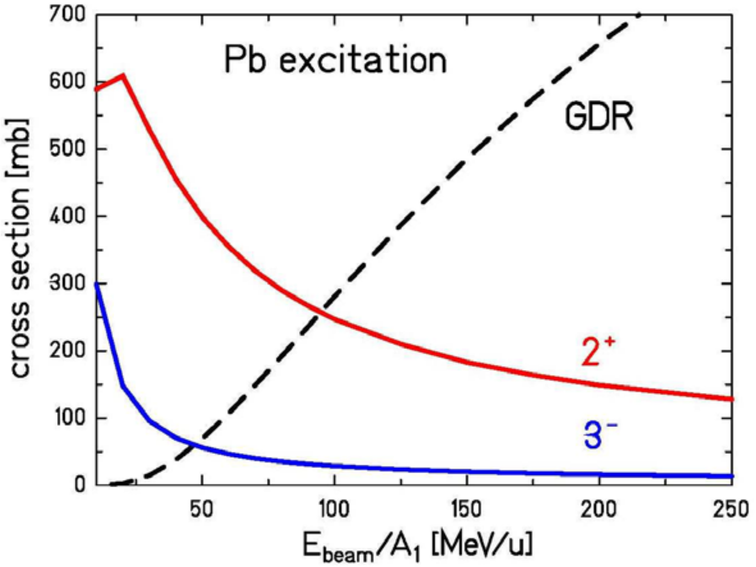

Rutherford scattering only if distance of closest approach D_{min} is large compared to nuclear radii + surfaces:

$$D_{\min} > C_P + C_T + 5\ \ fm$$

C_P, C_T half-density radii

$$\sigma_{\pi\lambda} \approx \left(\frac{Z_P e^2}{\hbar c}\right)^2 \cdot \frac{\pi}{e^2 b^{2\lambda-2}} \cdot B(\pi\lambda;0\to\lambda)\cdot\begin{cases}(\lambda-1)^{-1} & for\ \ \lambda\ge 2\\ 2\ln(b_a/b) & for\ \ \lambda=1\end{cases}$$

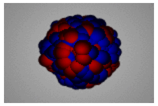

$E^* \cong 13.3\,MeV$

$B(E1;0\to 1^-) \cong 0.55\,e^2 b$

$E^* = 4.086\,MeV$

$B(E2;0\to 2^+) = 9\,Wu$

$E^* = 2.615\,MeV$

$B(E3;0\to 3^-) = 34\,Wu$

Atomic Background Radiation

➢Radiative electron capture (REC)
capture of target electrons into bound states of the projectile:

$$\sigma \sim Z_p^2 \cdot Z_t$$

➢Primary Bremsstrahlung (PB)
capture of target electrons into continuum states of the projectile:

$$\sigma \sim Z_p^2 \cdot Z_t$$

➢Secondary Bremsstrahlung (SB)
Stopping of high energy electrons in the target: $\sigma \sim Z_p^2 \cdot Z_t^2$

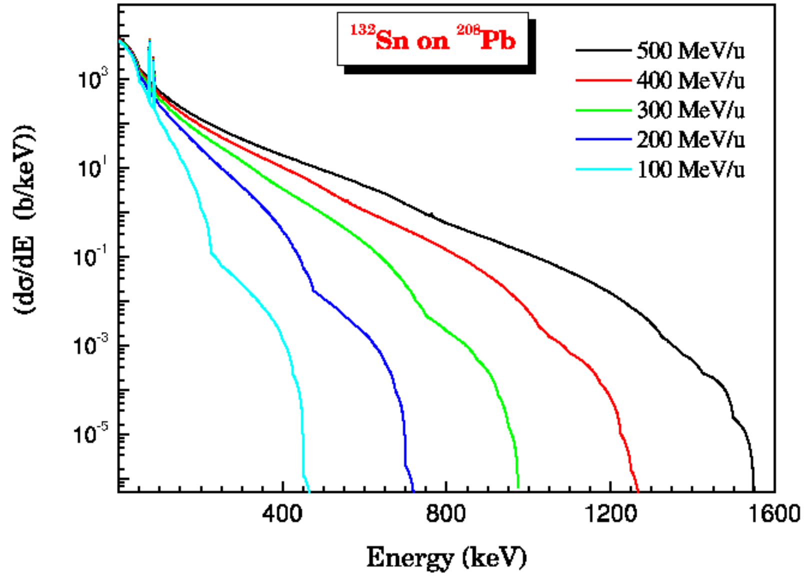

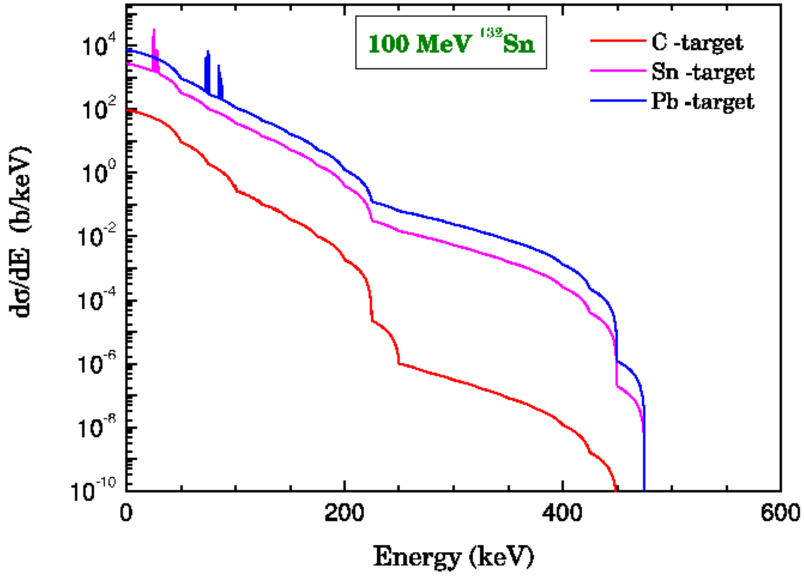

Bremsstrahlung: slowing down of a moving point-charge

Scattering Experiment at Relativistic Energies

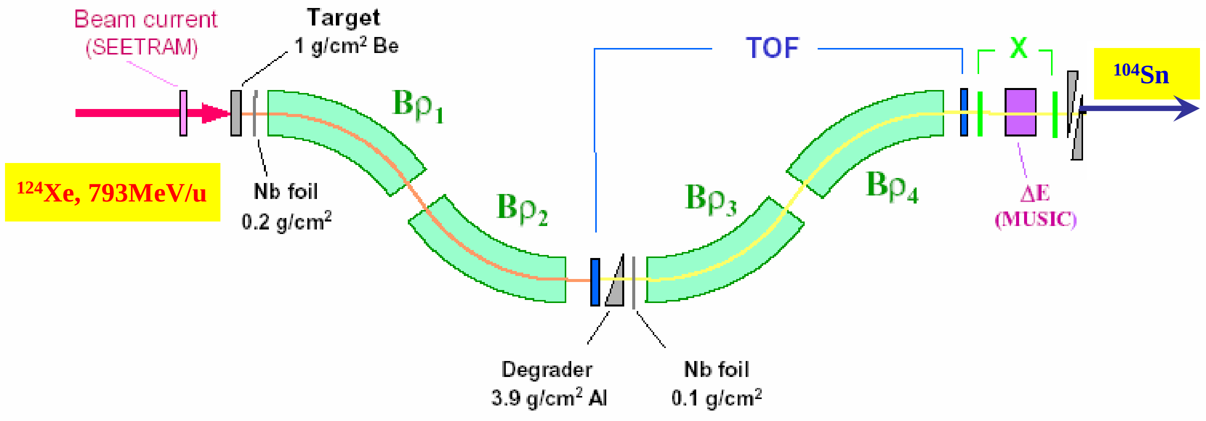

^{197}Au-target

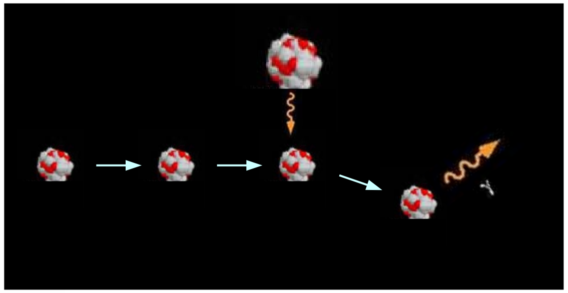

relativistic Coulomb excitation

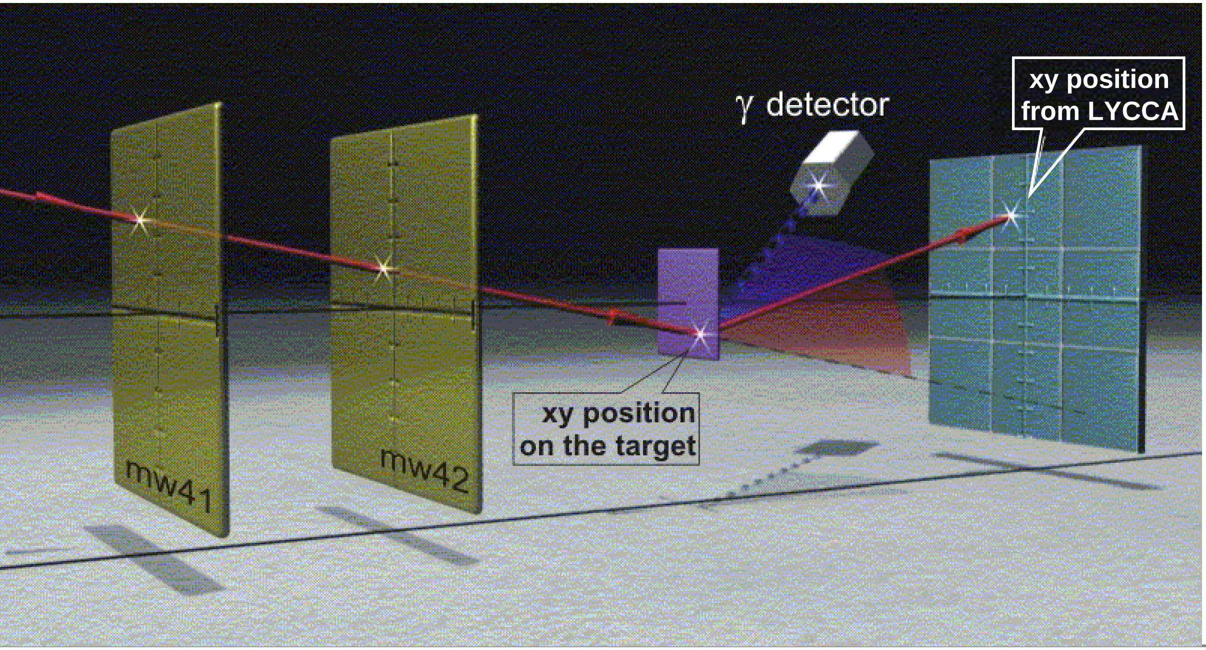

Scattering Experiment at Relativistic Energies

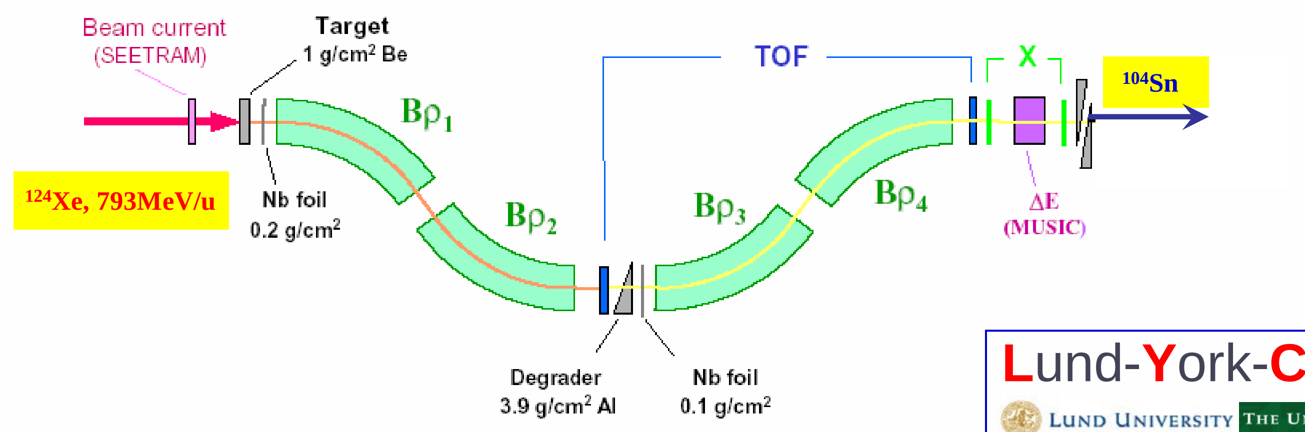

Lund-York-Cologne CAlorimeter

LUND UNIVERSITY — THE UNIVERSITY of York — University of Cologne

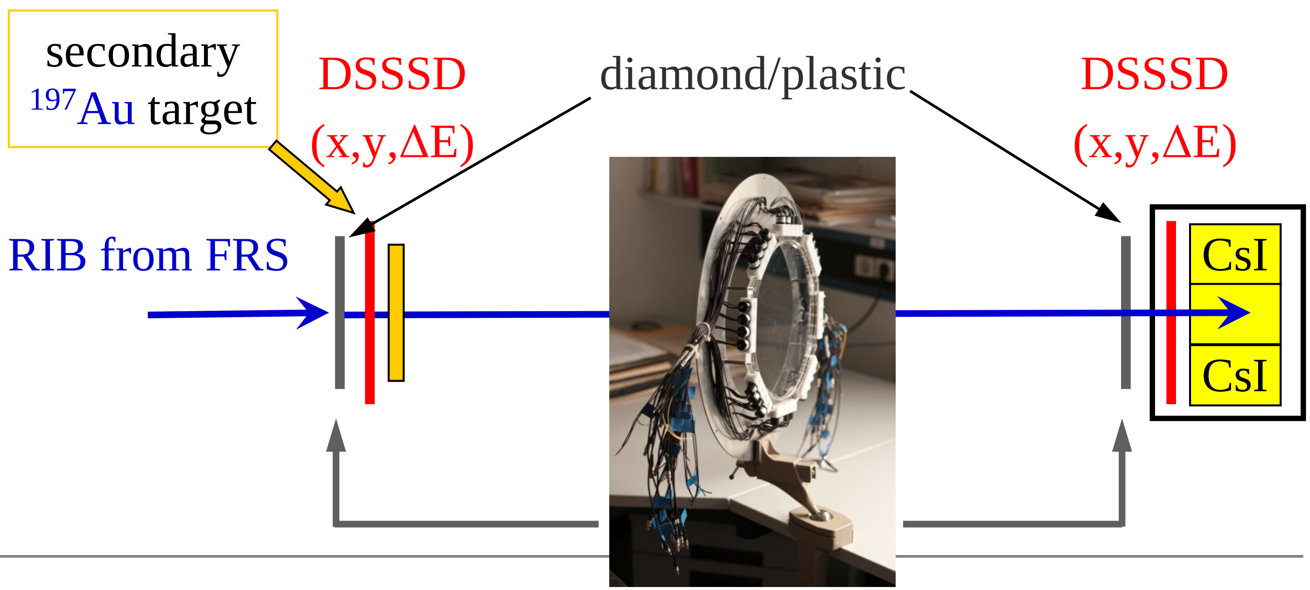

exp. observables:
Z, A, θ

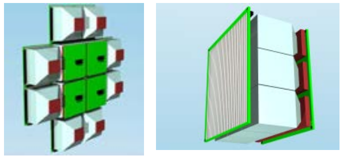

Scattering Experiment at Relativistic Energies

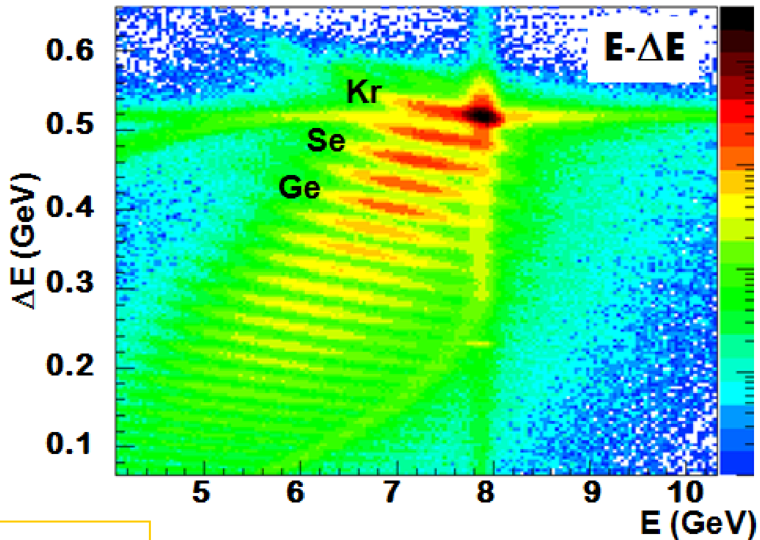

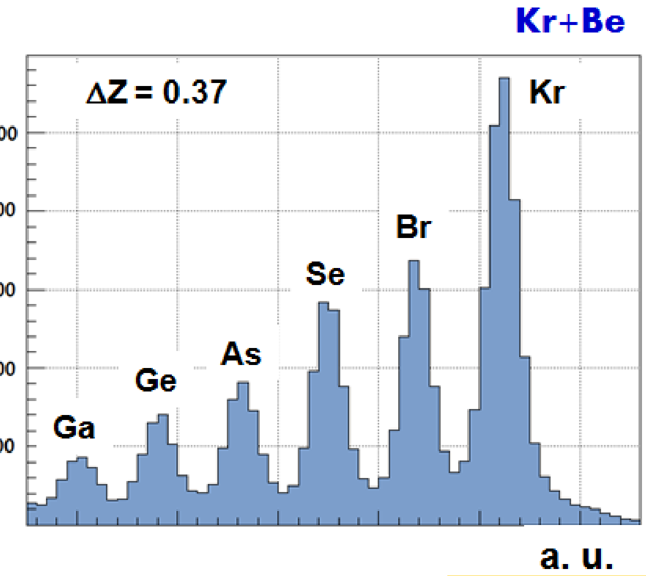

secondary
^{9}Be target

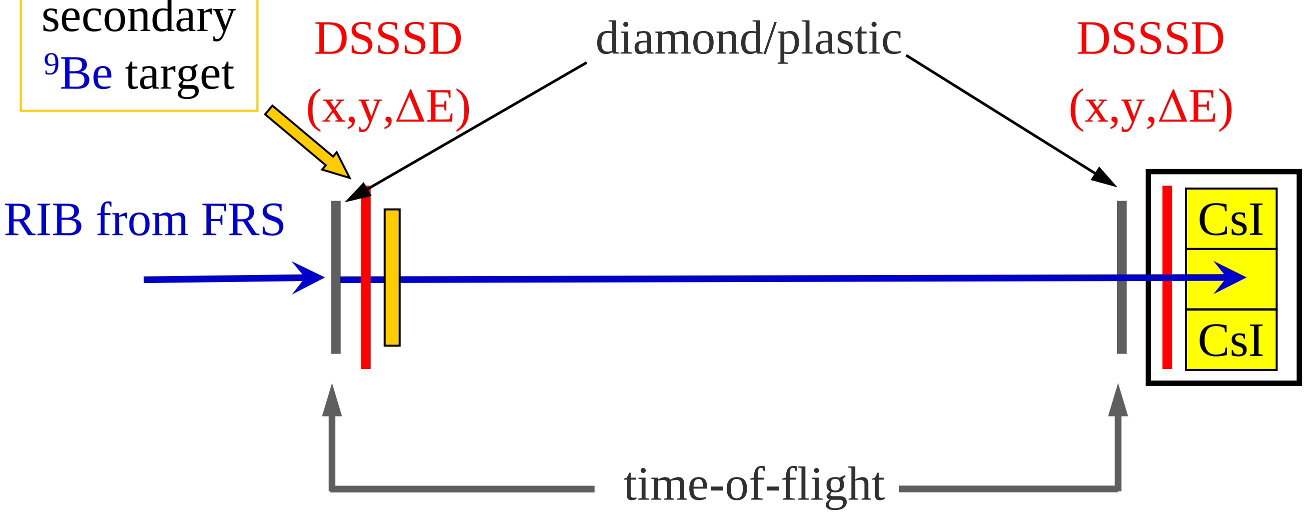

exp. observables:
Z, A, θ

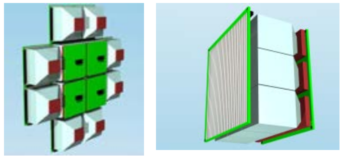

Scattering Experiment at Relativistic Energies

$$m \cdot c^2 = \frac{E_{kin}}{\gamma - 1}$$

with $E_{kin} = E_{CsI} + \Delta E_{DSSSD}$

and $\gamma = \frac{1}{\sqrt{1-\left(v/c\right)^2}}$

with v from LYCCA-ToF

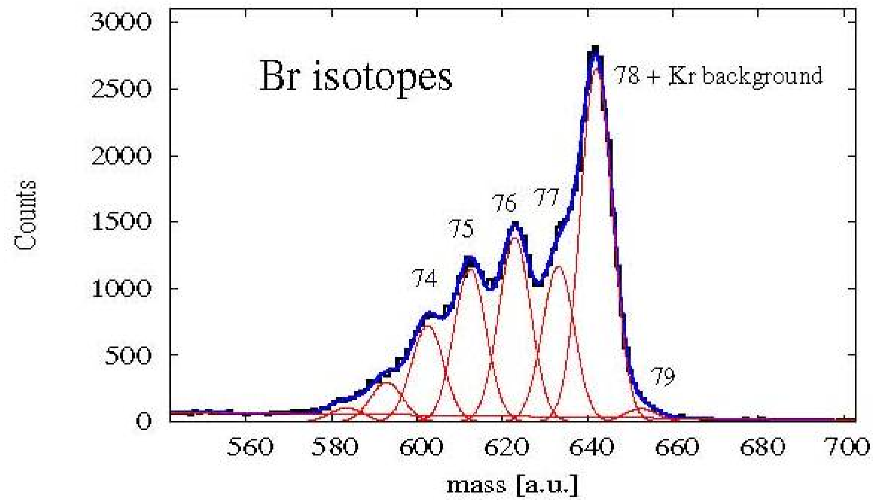

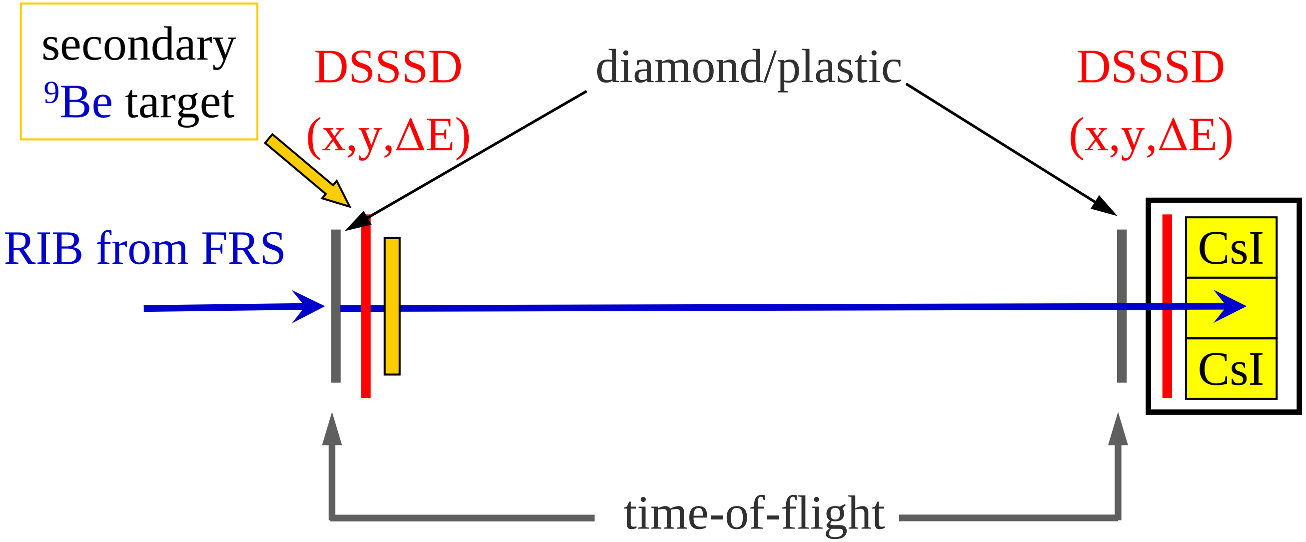

exp. observables:
Z, **A**, **θ**

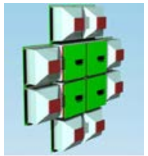

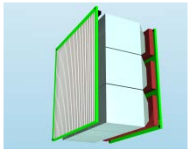

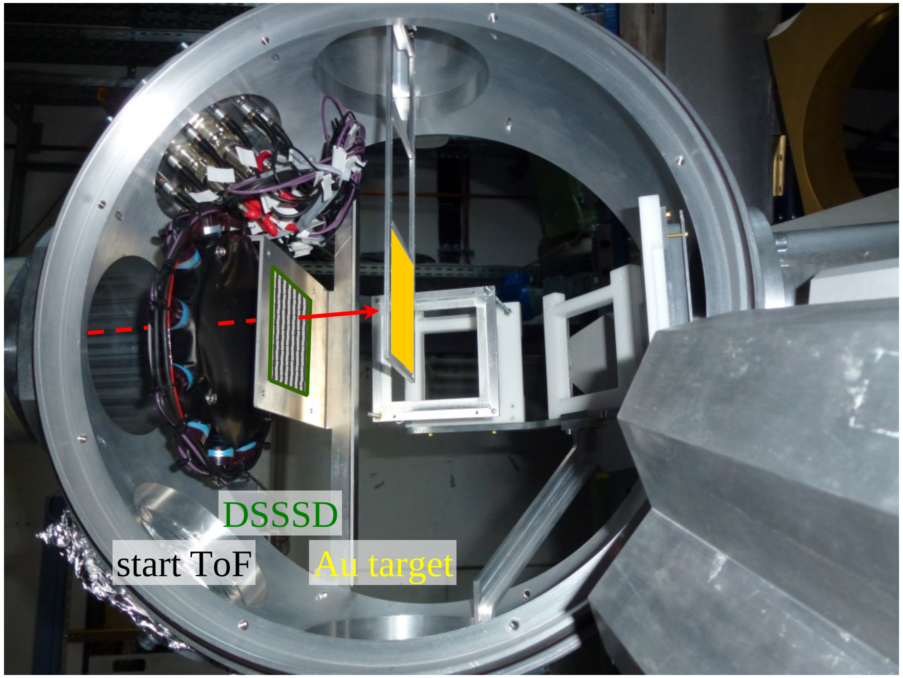

PreSPEC target chamber

variable target position (13cm, 23cm)

Additional γ-Ray Background Radiation

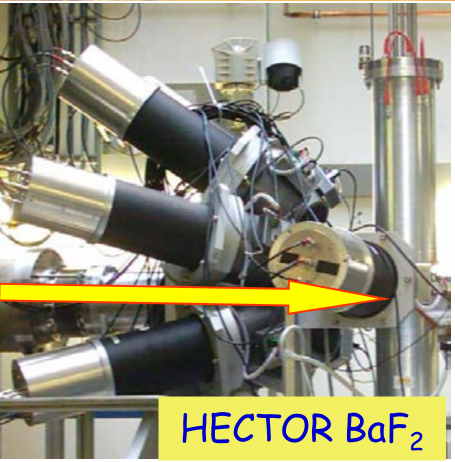

^{37}Ca beam
at 196 MeV/u

Coulomb excitation:
A/Q - ^{37}Ca
all Ca detected in **ΔE-E**

1‰ interaction target
most γ-rays from CATE

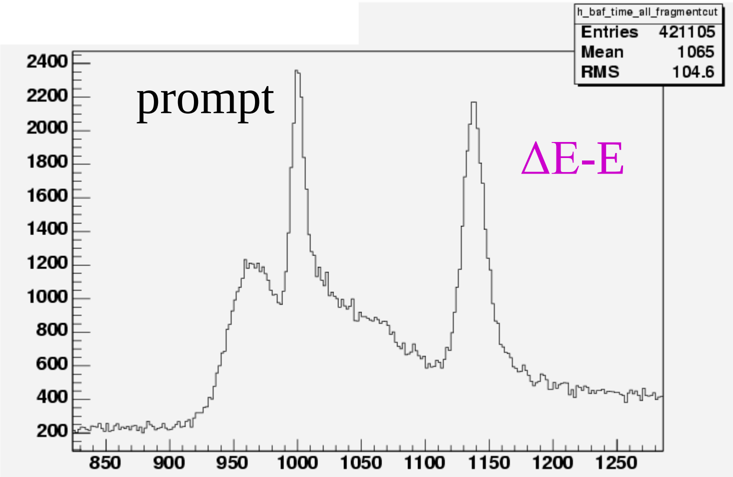

time spectrum

Fragmentation:
A/Q - ^{37}Ca
K detected (mainly ^{36}K)

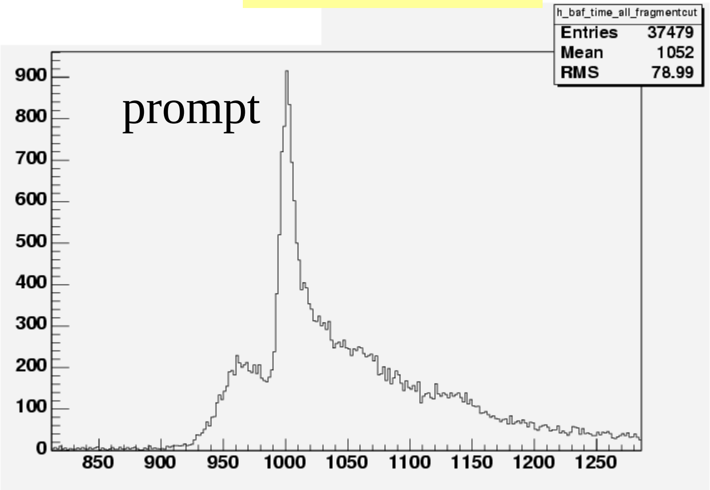

Scattering Experiment at Relativistic Energies

^{80}Kr $\rightarrow$ ^{197}Au, 150 AMeV

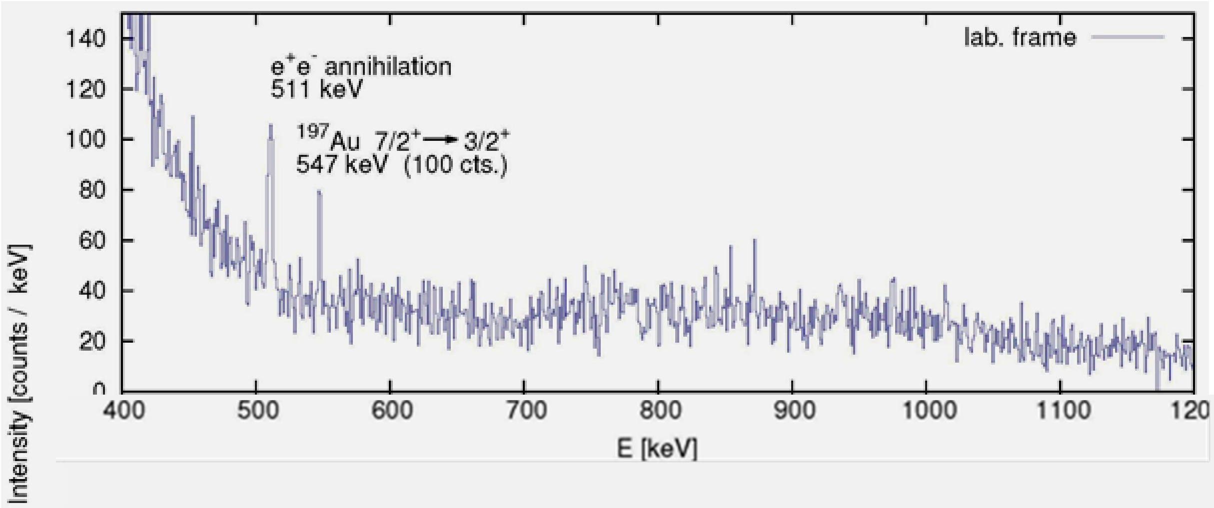

Doppler effect

$$\frac{E_{\gamma 0}}{E_\gamma} = \frac{1-\beta \cdot \cos \vartheta_\gamma^{\ell ab}}{\sqrt{1-\beta^2}}$$

Scattering Experiment at Relativistic Energies

Doppler effect:

$$\frac{E_{\gamma 0}}{E_{\gamma}} = \frac{1-\beta\cdot\cos\vartheta_{\gamma}^{\ell ab}}{\sqrt{1-\beta^2}} \qquad \text{for } \vartheta_p \cong 0^0$$

Lorentz boost:

$$\frac{d\Omega_{rest}}{d\Omega_{lab}} = \left(\frac{E_{\gamma}}{E_{\gamma 0}}\right)^2$$

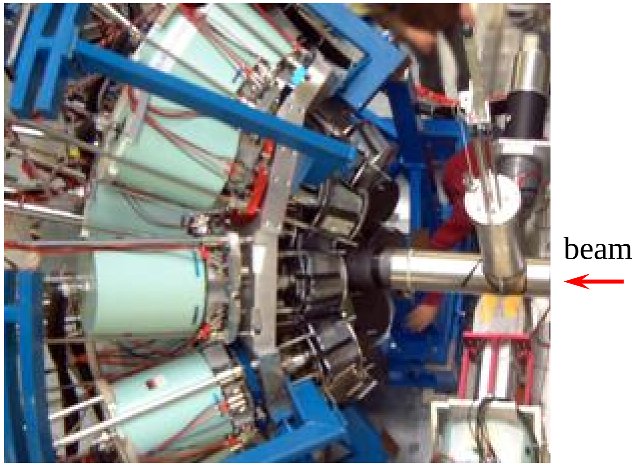

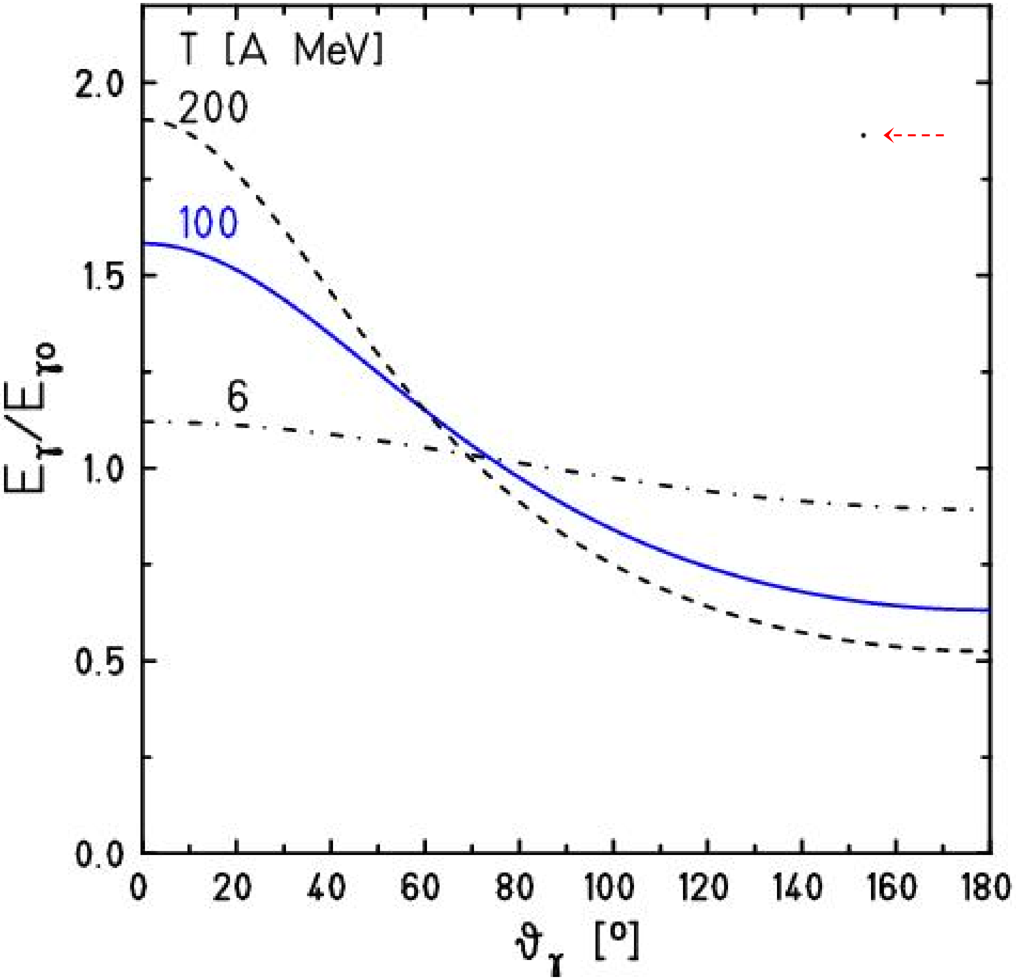

Doppler-Shift Correction

^{238}U on ^{197}Au (386 mg/cm^2) at 183 AMeV

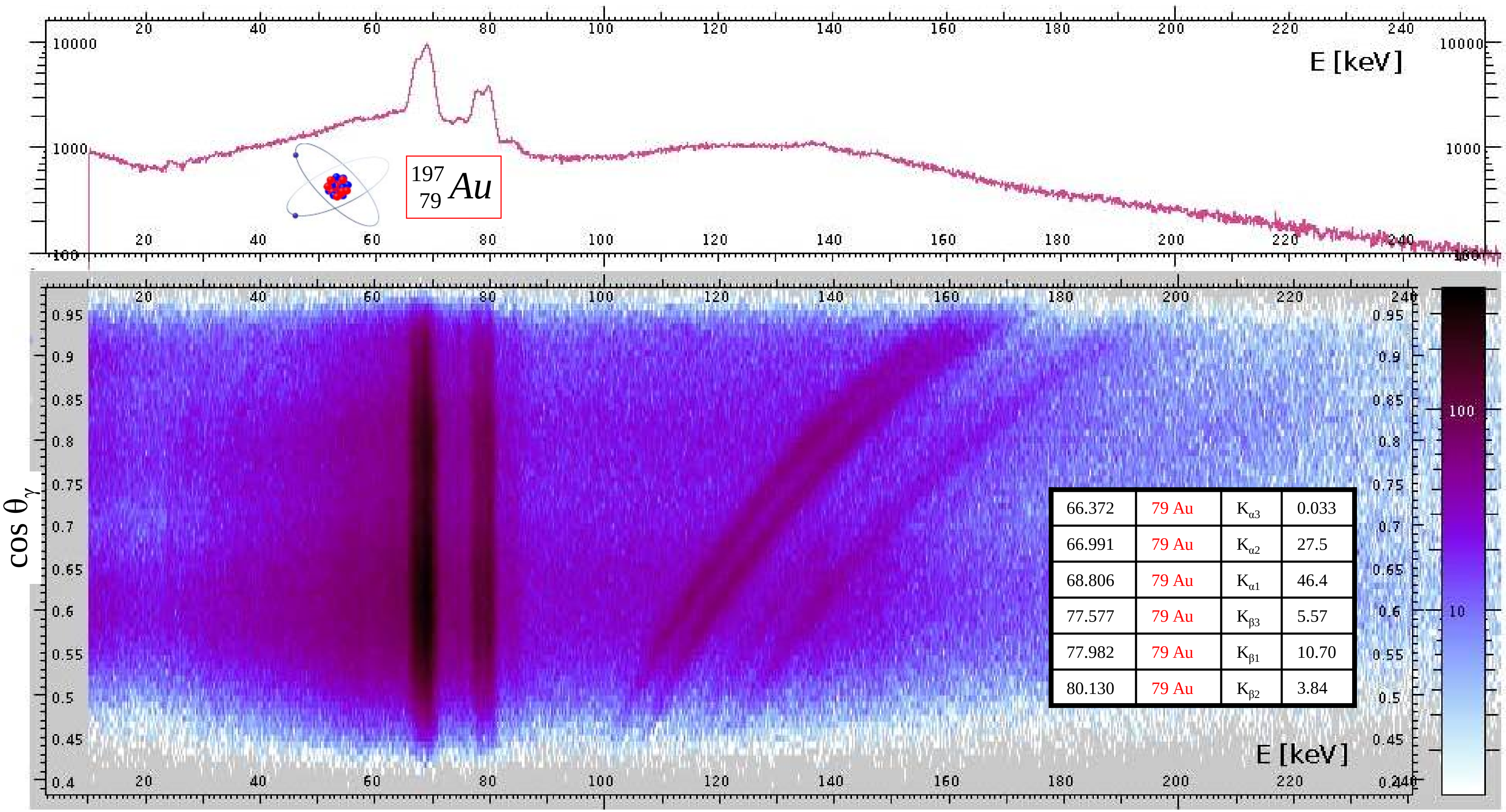

66.372	79 Au	$K_{\alpha 3}$	0.033
66.991	79 Au	$K_{\alpha 2}$	27.5
68.806	79 Au	$K_{\alpha 1}$	46.4
77.577	79 Au	$K_{\beta 3}$	5.57
77.982	79 Au	$K_{\beta 1}$	10.70
80.130	79 Au	$K_{\beta 2}$	3.84

Doppler-Shift Correction

^{238}U on ^{197}Au (386 mg/cm^2) at 183 AMeV

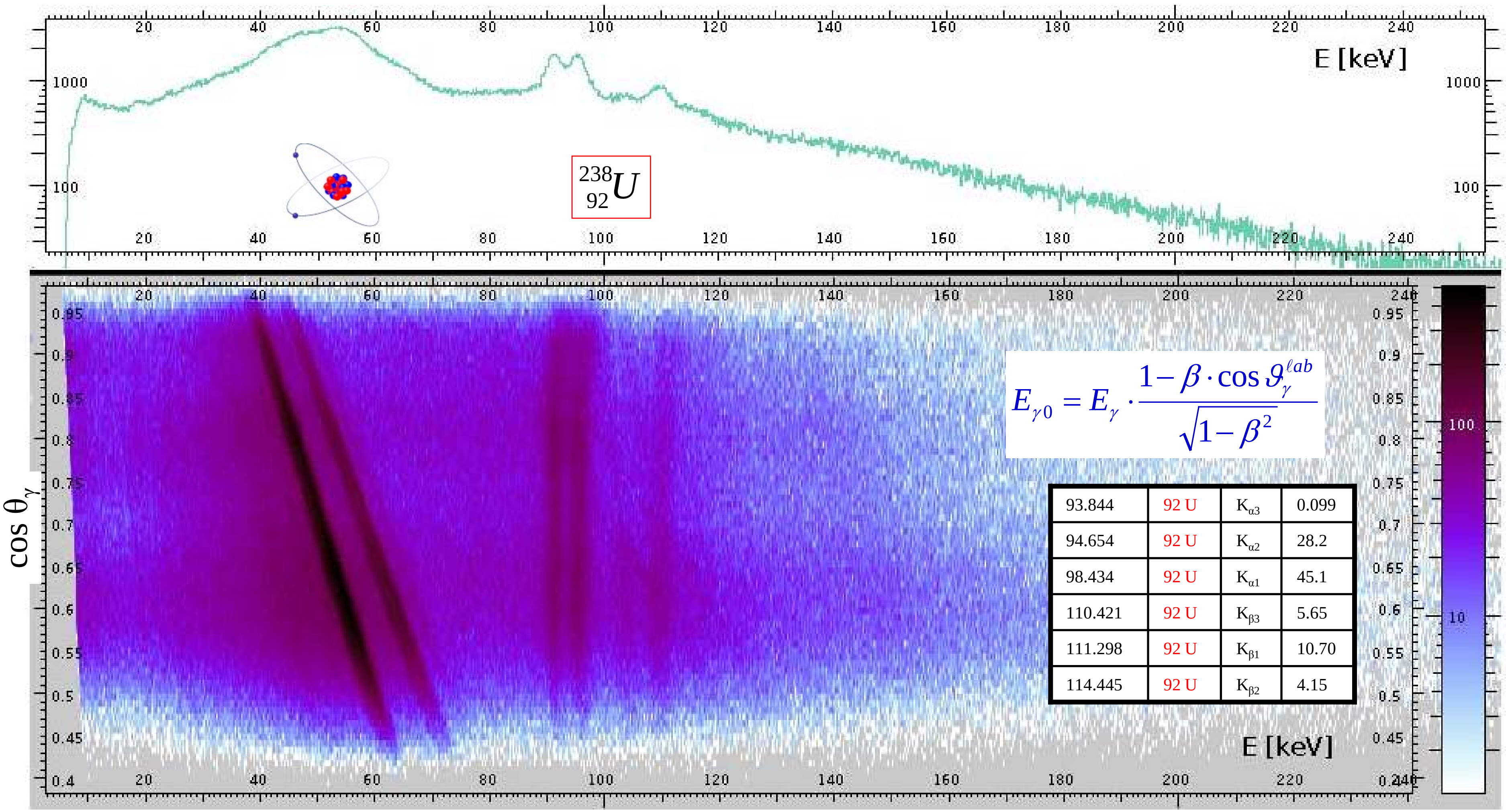

$$E_{\gamma 0} = E_\gamma \cdot \frac{1-\beta \cdot \cos \vartheta_\gamma^{\ell ab}}{\sqrt{1-\beta^2}}$$

93.844	92 U	$K_{\alpha 3}$	0.099
94.654	92 U	$K_{\alpha 2}$	28.2
98.434	92 U	$K_{\alpha 1}$	45.1
110.421	92 U	$K_{\beta 3}$	5.65
111.298	92 U	$K_{\beta 1}$	10.70
114.445	92 U	$K_{\beta 2}$	4.15

Doppler Broadening

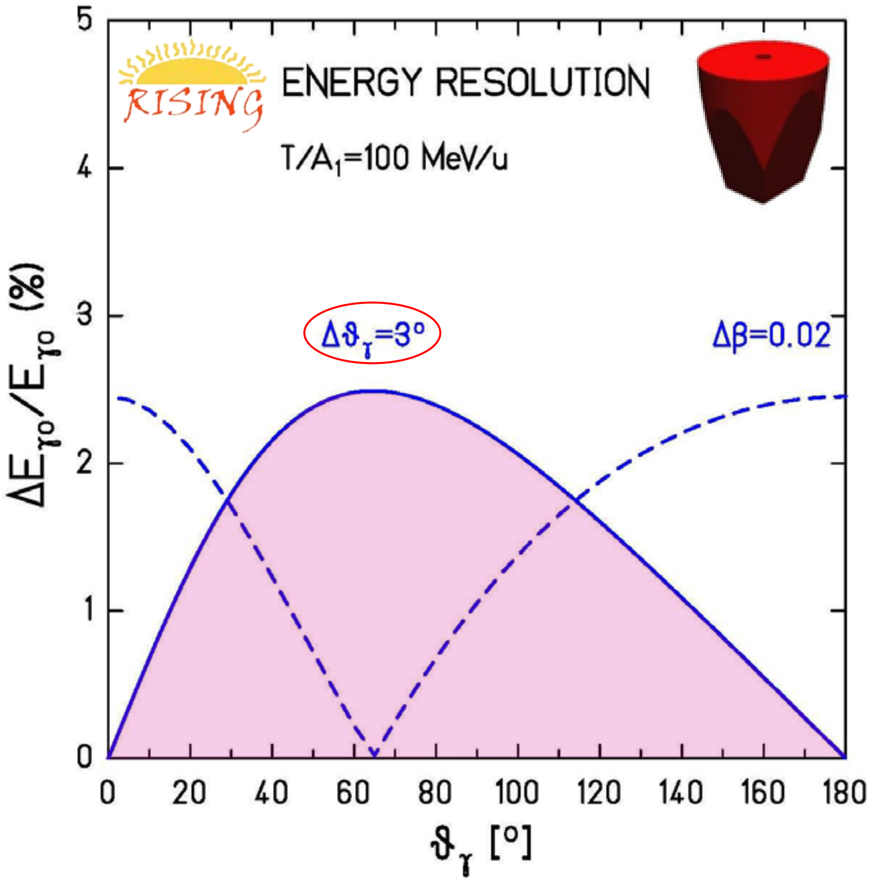

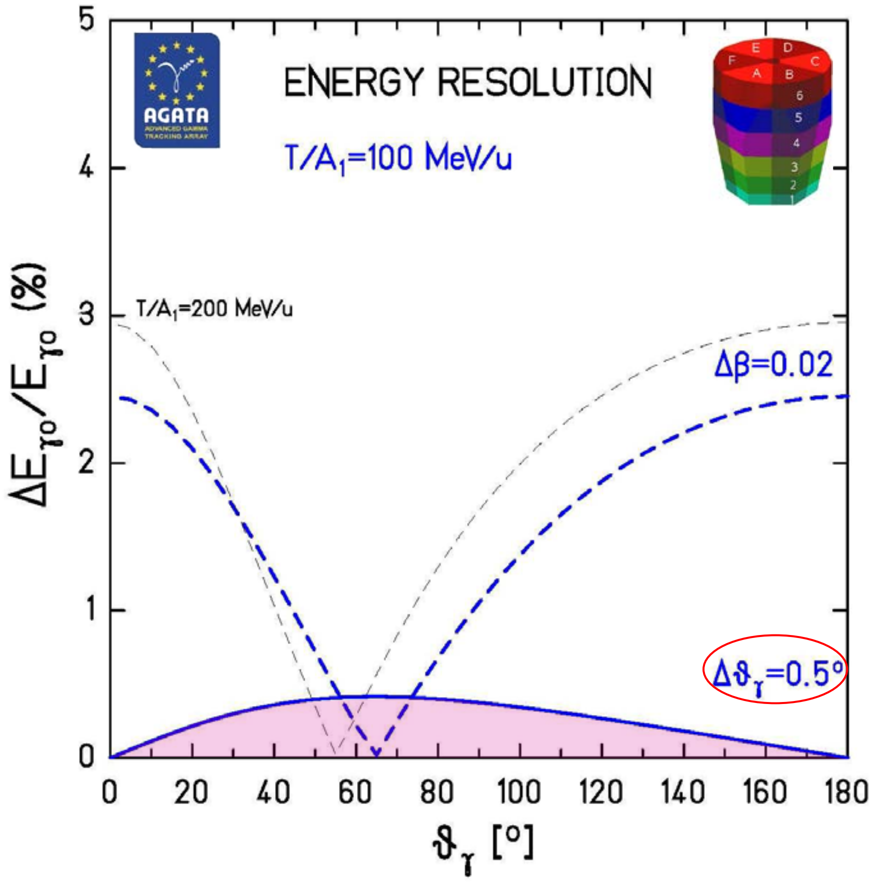

opening angle:

$$\frac{\Delta E_{\gamma 0}}{E_{\gamma 0}} = \frac{\beta \cdot \sin \vartheta_\gamma}{1 - \beta \cdot \cos \vartheta_\gamma} \cdot \Delta \vartheta_\gamma$$

slowing down in target:

$$\frac{\Delta E_{\gamma 0}}{E_{\gamma 0}} = \frac{\beta - \cos \vartheta_\gamma}{(1-\beta^2) \cdot (1 - \beta \cdot \cos \vartheta_\gamma)} \cdot \Delta \beta$$

γ-ray set-up with higher efficiency

Advanced GAmma Tracking Array

Encapsulation

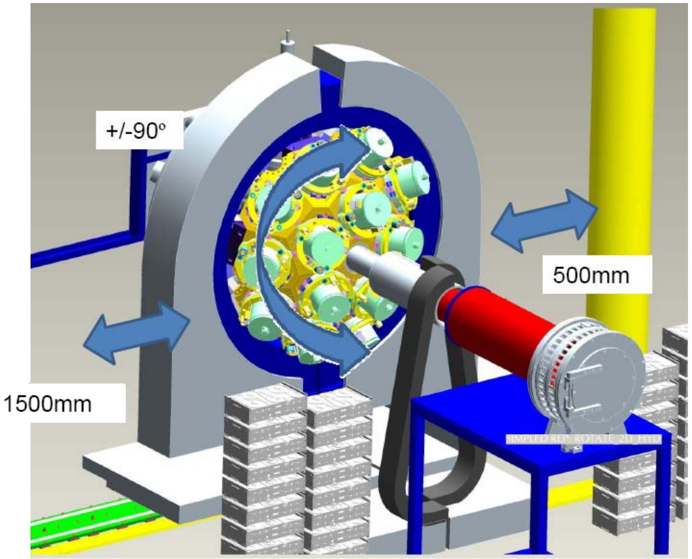

John Strachan

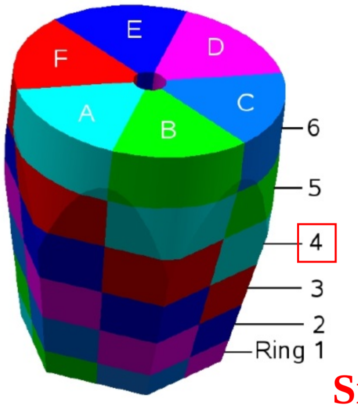

Signals from 36 segments + core are measured as a function of time (γ-ray interaction point)

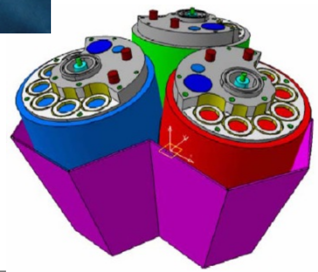

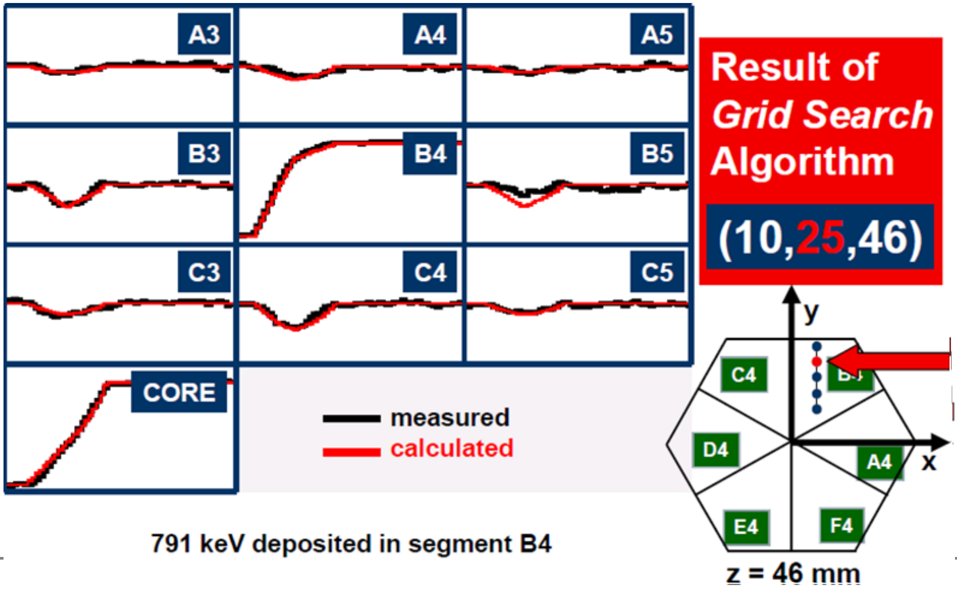

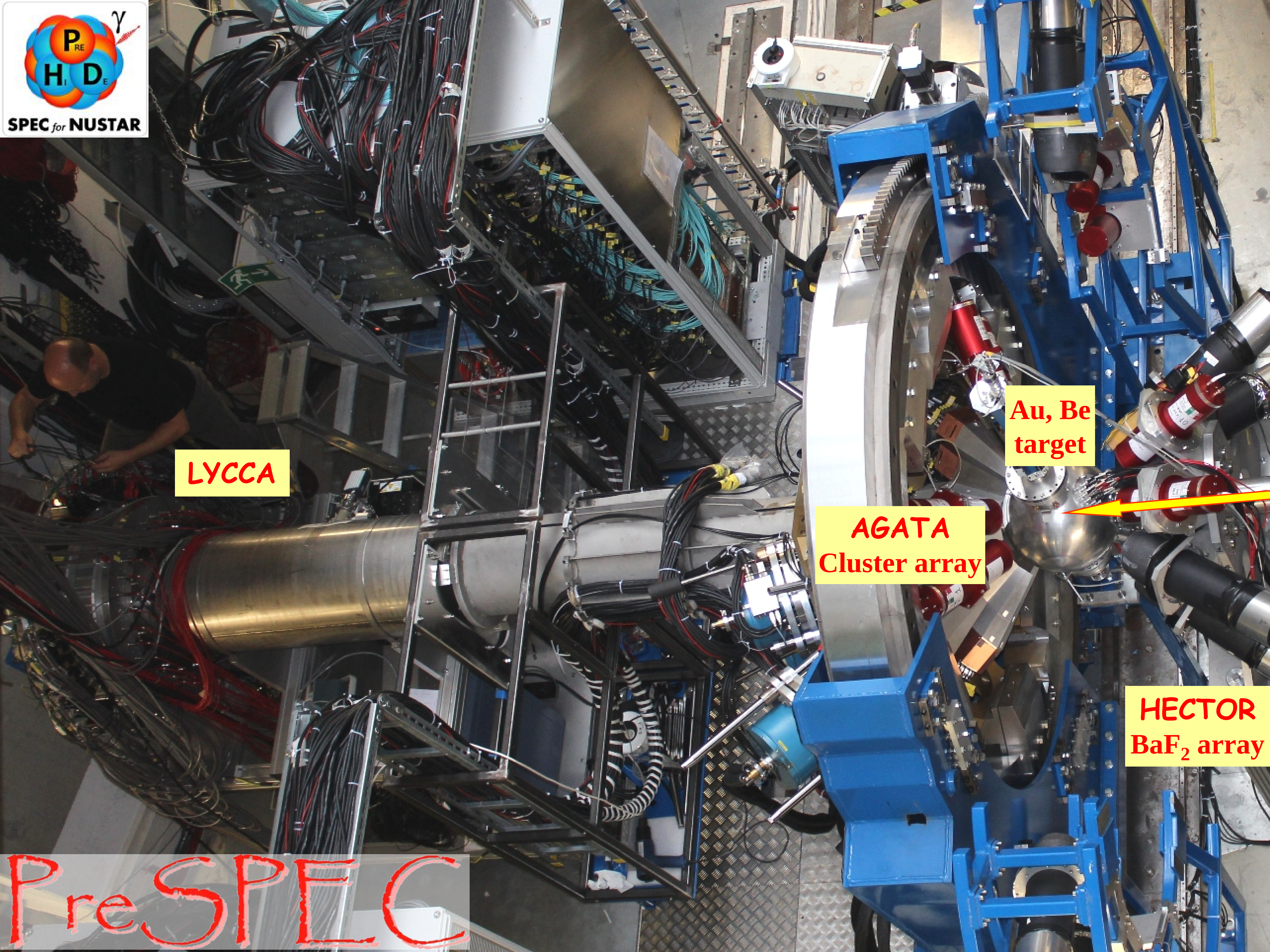
SPEC for NUSTAR
LYCCA
Au, Be target
AGATA Cluster array
HECTOR BaF$_2$ array
PreSPEC

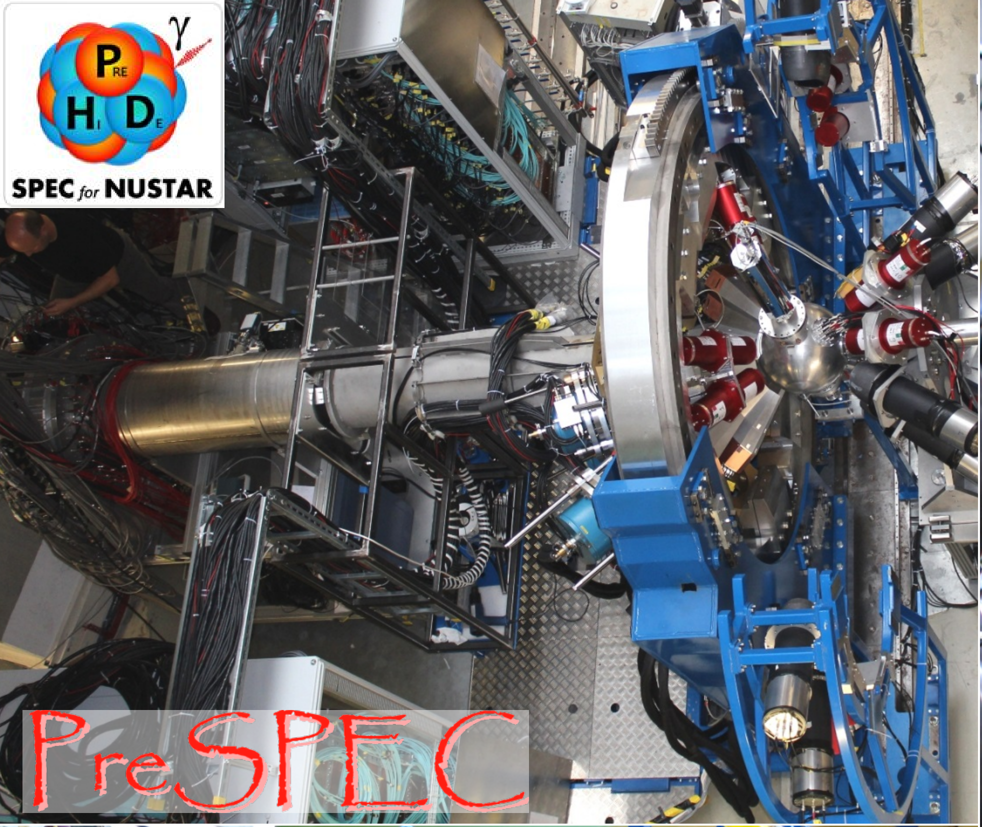
SPEC for NUSTAR
PreSPEC
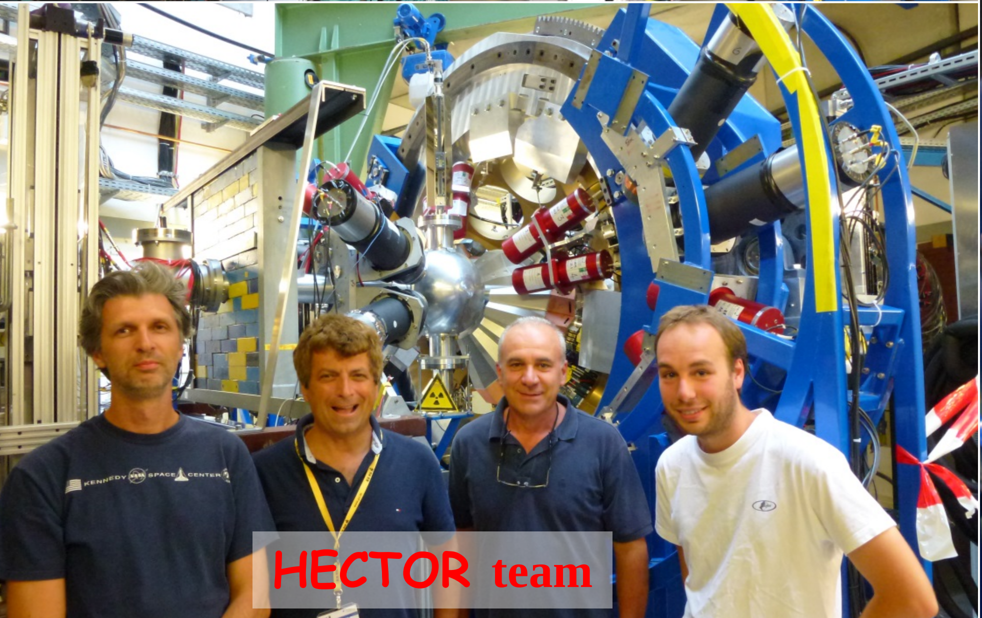
HECTOR team
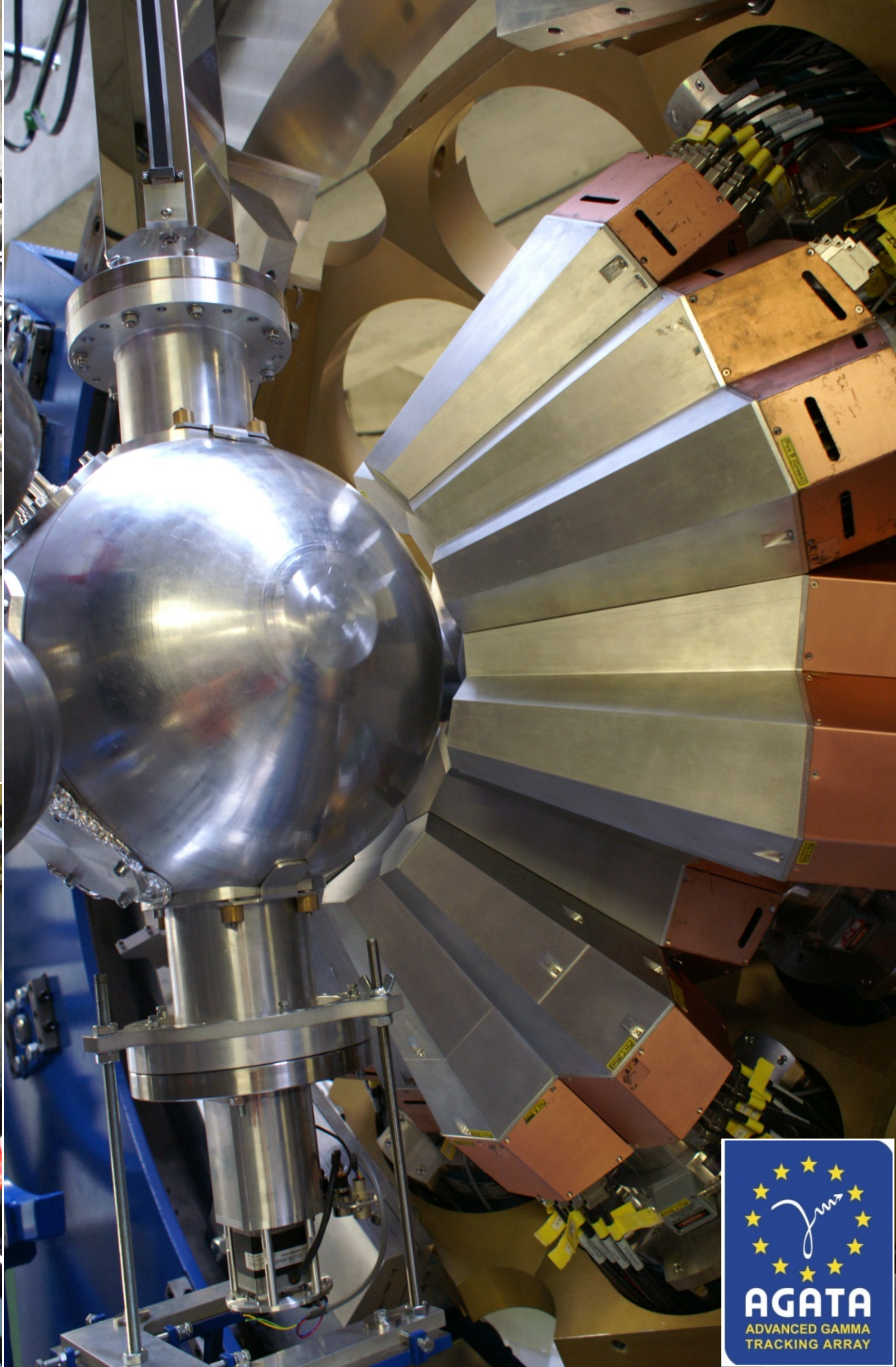
AGATA
ADVANCED GAMMA
TRACKING ARRAY

AGATA at PreSPEC

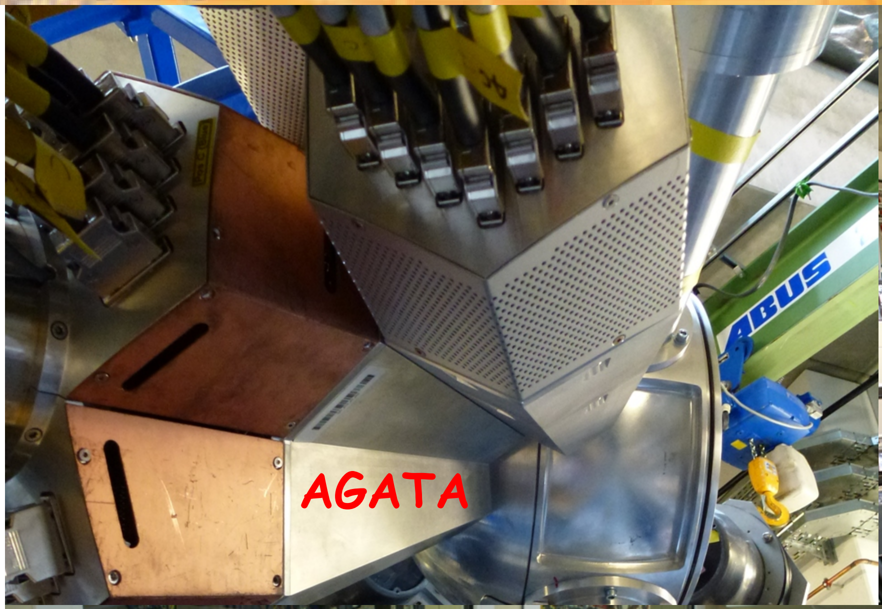

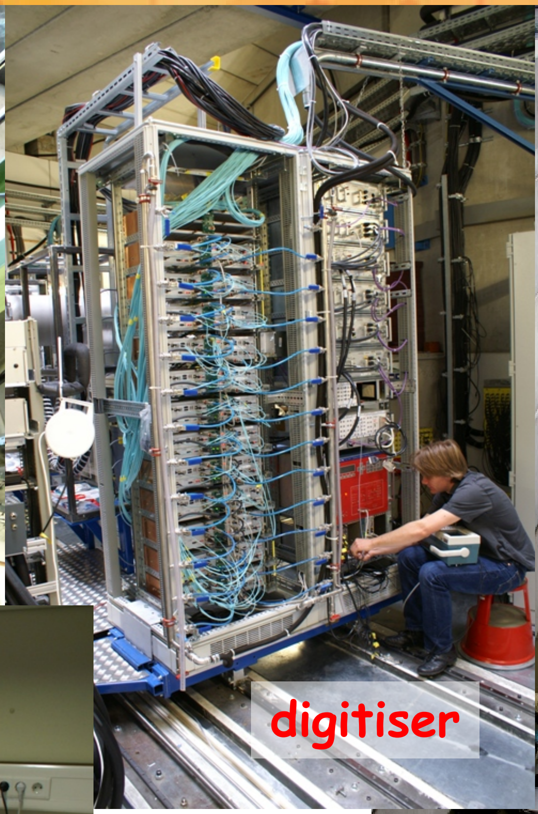

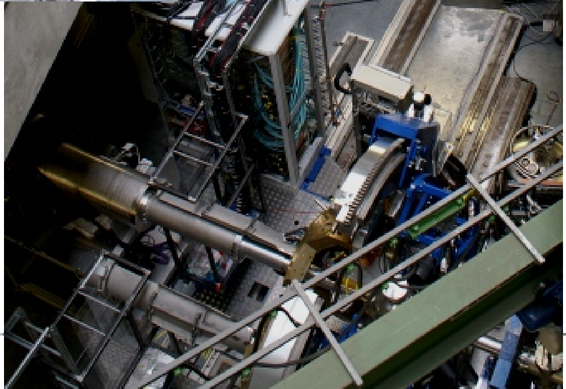

Damian Ralet,
Stephane Pietri

High-energy Coulomb excitation

triaxiality in even-even nuclei (N=76)

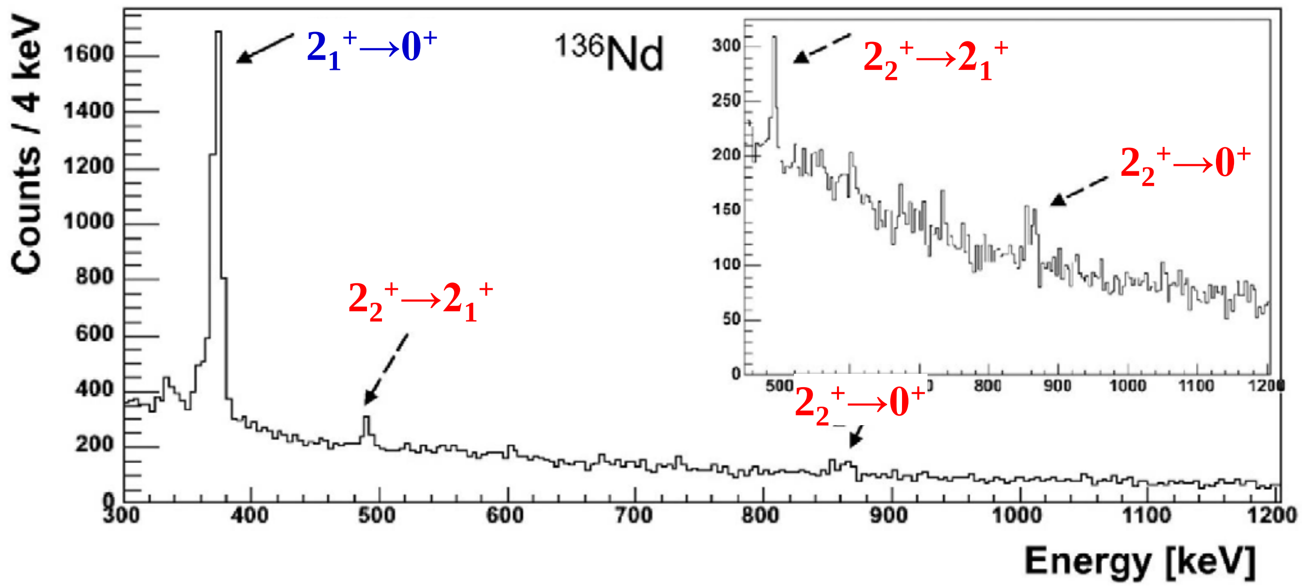

First observation of a second excited 2$^+$ state
populated in a Coulomb experiment at 100 AMeV using EUROBALL and MINIBALL Ge-detectors.

- shape symmetry
- collective strength

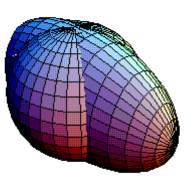

$$\frac{B(E2;2_2 \rightarrow 2_1)}{B(E2;2_1 \rightarrow 0)} = \frac{\frac{20}{7}\frac{\sin^2(3\gamma)}{9-8\sin^2(3\gamma)}}{1+\frac{3-2\sin^2(3\gamma)}{\sqrt{9-8\sin^2(3\gamma)}}}$$

$$\frac{B(E2;2_2 \rightarrow 0)}{B(E2;2_1 \rightarrow 0)} = \frac{1-\frac{3-2\sin^2(3\gamma)}{\sqrt{9-8\sin^2(3\gamma)}}}{1+\frac{3-2\sin^2(3\gamma)}{\sqrt{9-8\sin^2(3\gamma)}}}$$

$$\frac{E_2(2)}{E_1(2)} = \frac{3+\sqrt{9-8\sin^2 3\gamma}}{3-\sqrt{9-8\sin^2 3\gamma}}$$

T.R. Saito et al. Phys.Lett. B669 (2008), 19

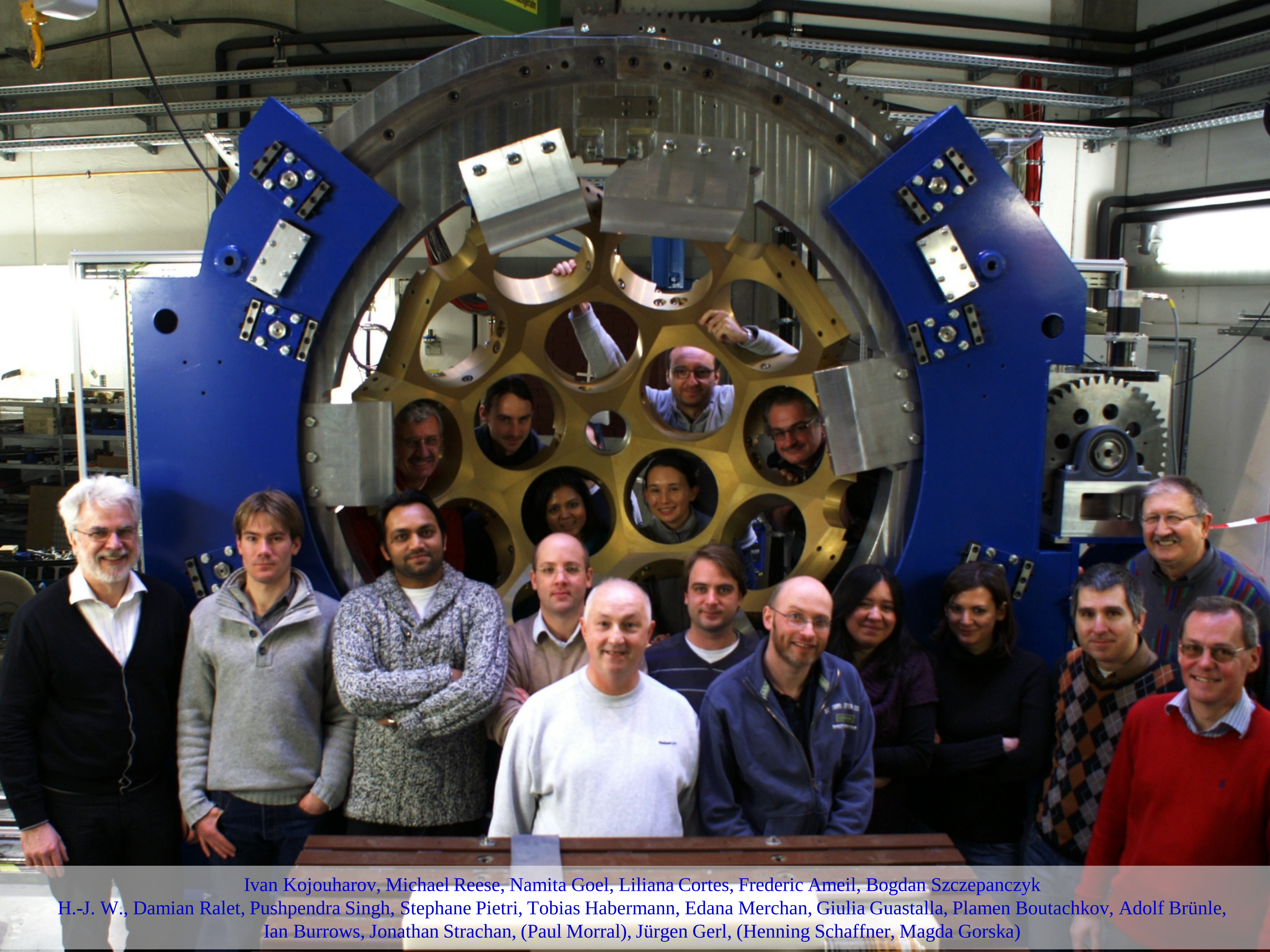

Ivan Kojouharov, Michael Reese, Namita Goel, Liliana Cortes, Frederic Ameil, Bogdan Szczepanczyk
H.-J. W., Damian Ralet, Pushpendra Singh, Stephane Pietri, Tobias Habermann, Edana Merchan, Giulia Guastalla, Plamen Boutachkov, Adolf Brünle,
Ian Burrows, Jonathan Strachan, (Paul Morral), Jürgen Gerl, (Henning Schaffner, Magda Gorska)

Slowed down beams – new experimental perspectives

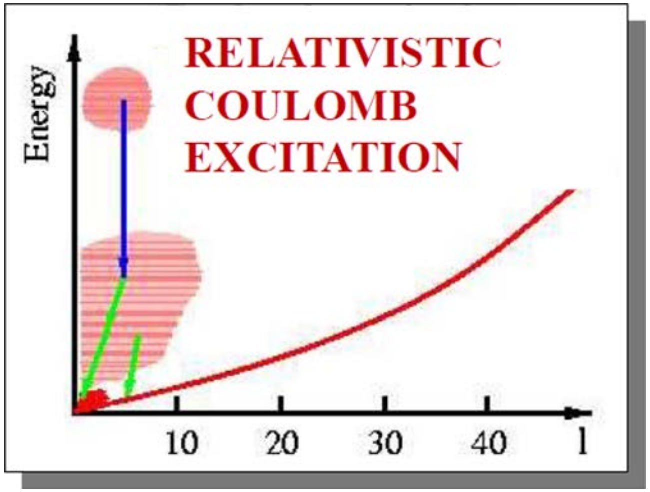

collective strength

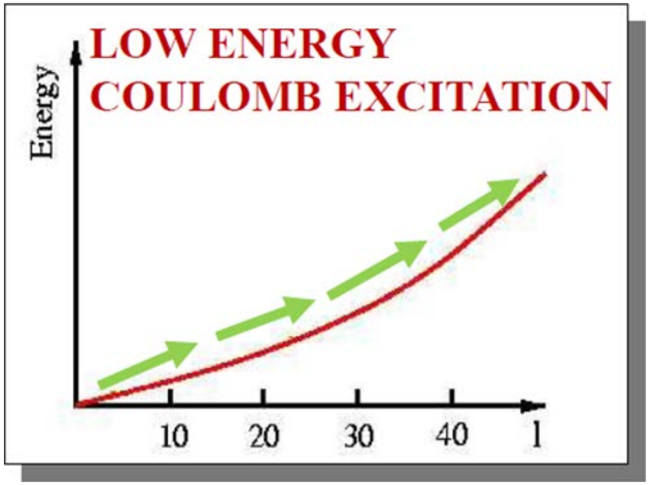

nuclear shape

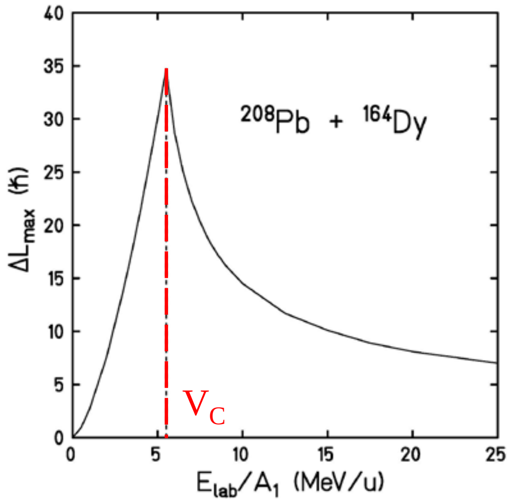

angular momentum transfer:

$$\Delta L_{\max} \cong \frac{Z_P \cdot e^2 \cdot Q_0}{4 \cdot \hbar \cdot v \cdot a^2} \cdot (1 - \cos\theta_{cm})$$

FAIR GSI

Slowed down beams – beam characteristics

10^9 pps	10^7 pps	$3 \cdot 10^6$ pps	10^5 pps

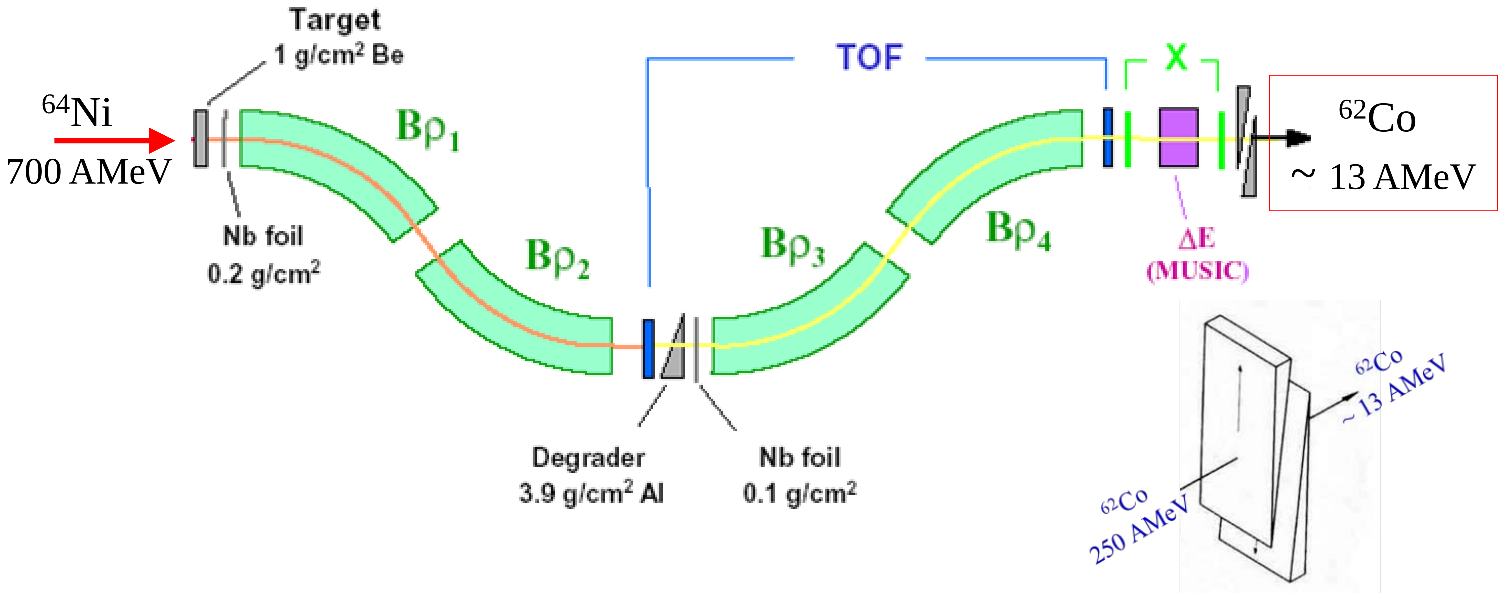

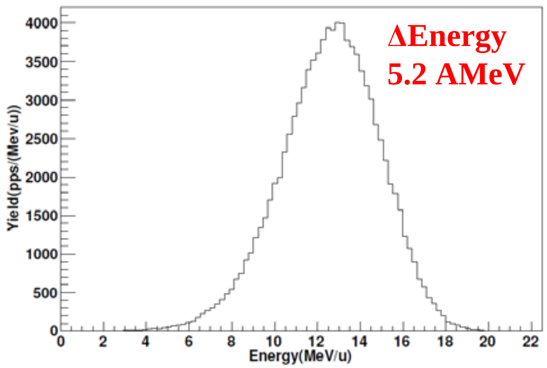

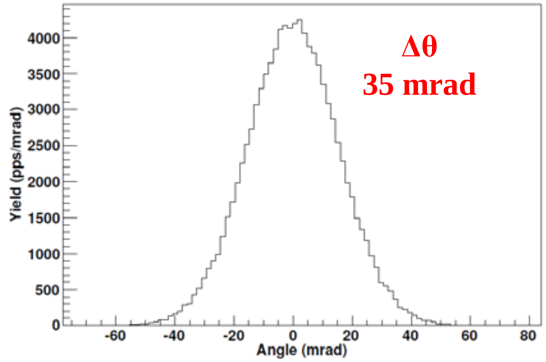

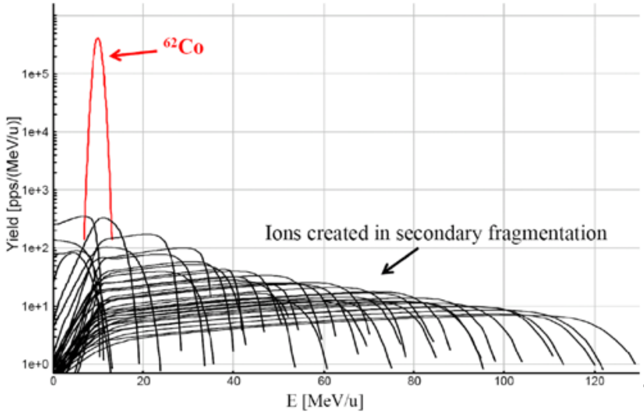

Slowed down beams – experimental set-up

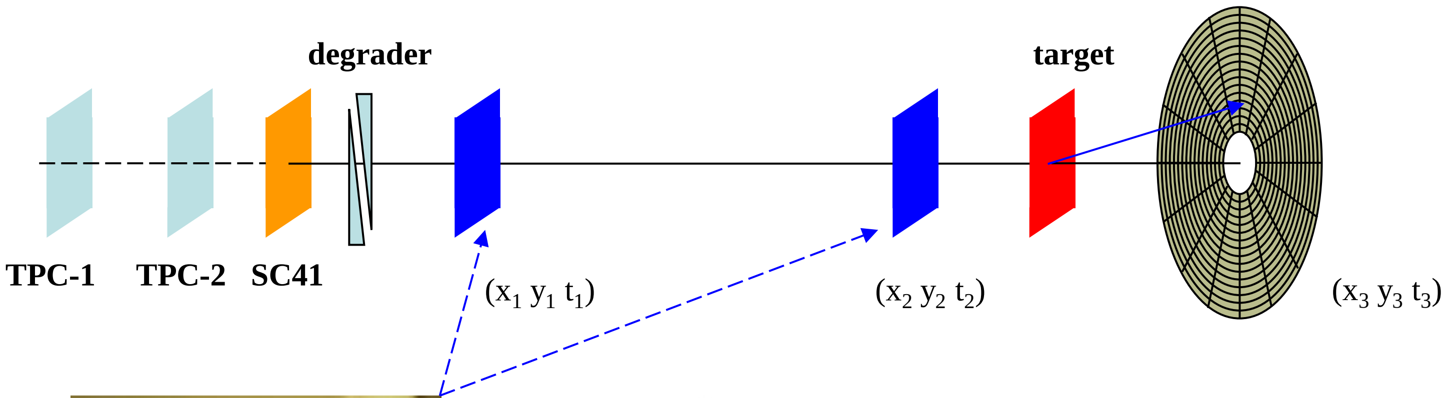

electrostatic mirror + MCP detector

position resolution ~ 1 mm
time resolution ~ 100 ps

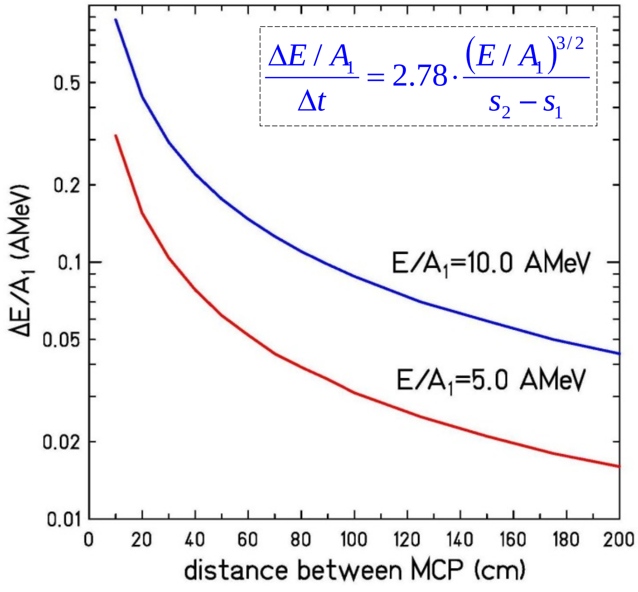

experimental results:

velocity β
beam energy E/A_1
scattering angle θ_{cm}

Slowed down beams – experimental set-up

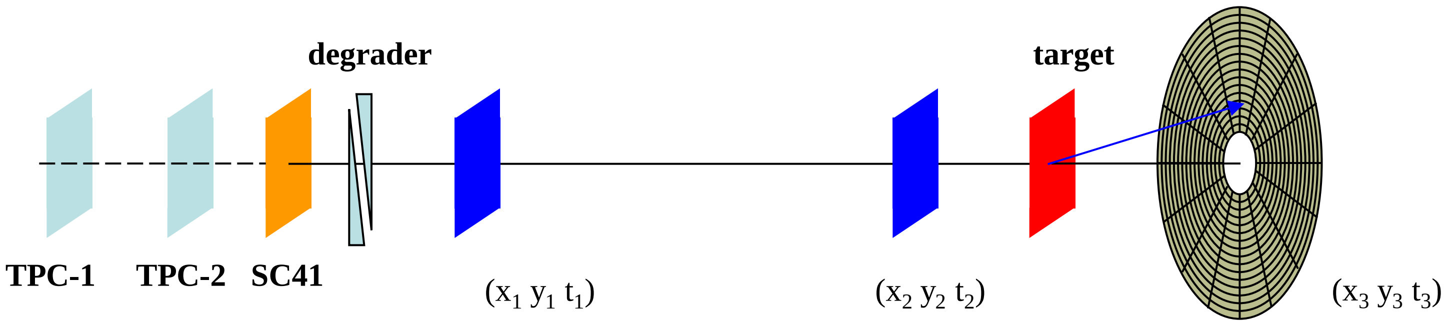

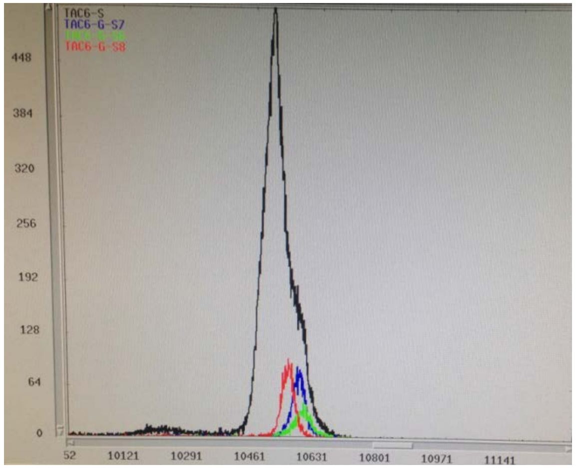

TOF between MCP and DSSSD

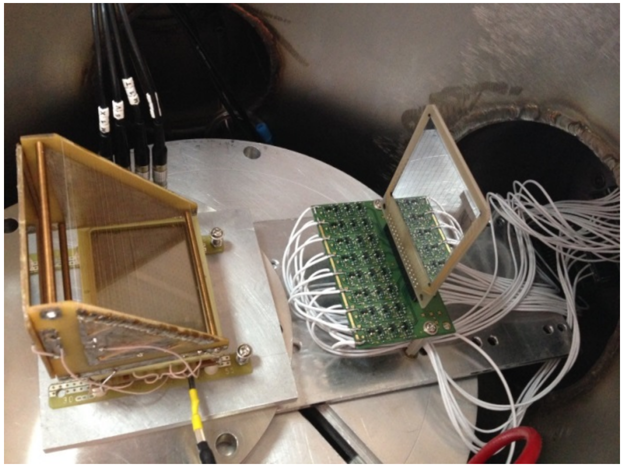

MCP DSSSD

Time resolution 200 ps for one of the 256 detector pixels

Akhil Jhingan (IUAC)

FAIR GSI

Reactions with Relativistic Radioactive Beams – R^3B

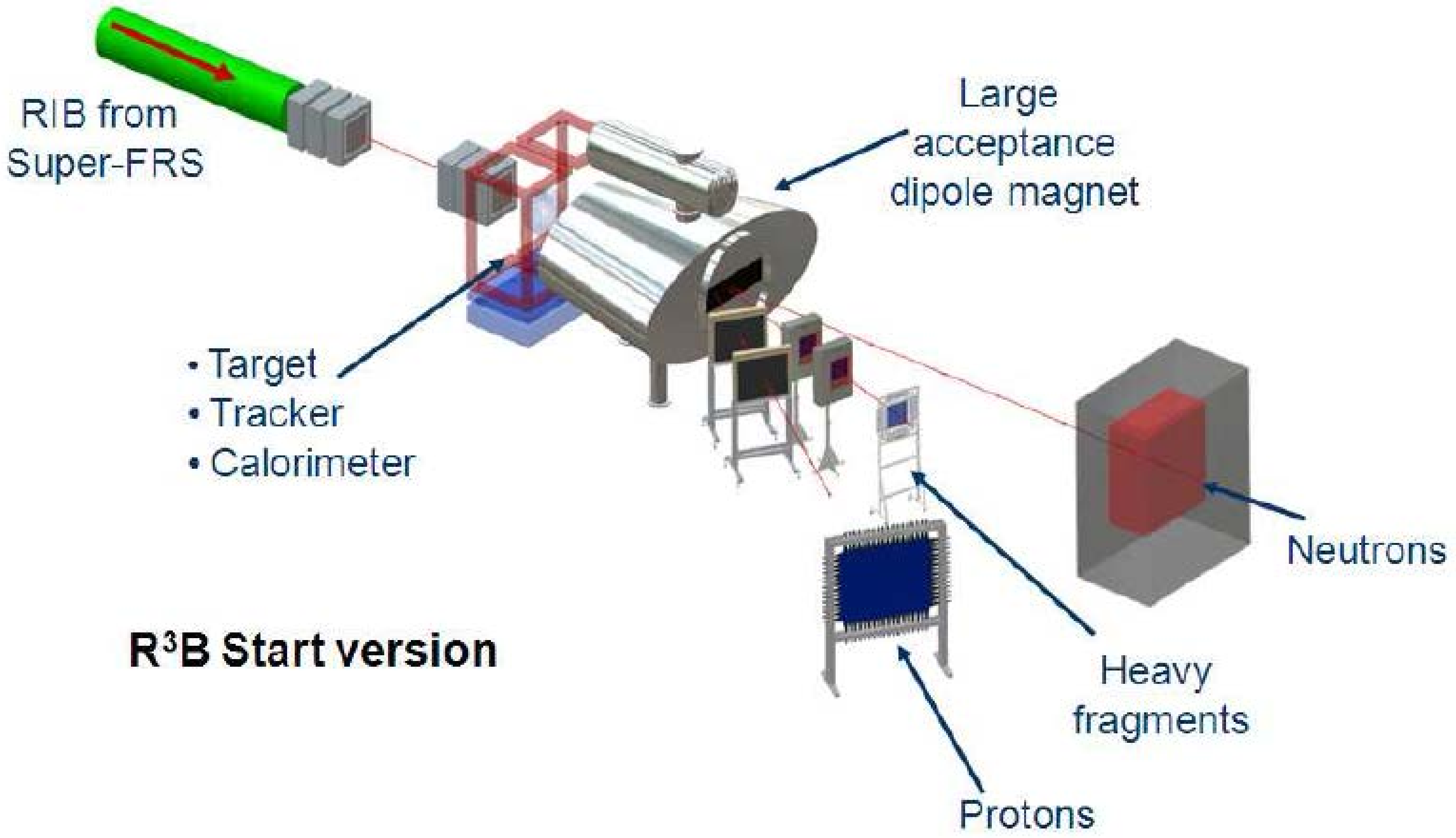

Excitation energy E^* from kinematically complete measurement of all outgoing particles

$$E^* = \left(\sqrt{\sum_i {m_i}^2 + \sum_{i \neq j} m_i m_j \gamma_i \gamma_j (1 - \beta_i \beta_j cos\vartheta_{ij})} - m_{proj} \right) c^2 + E_{\gamma,sum}$$

Dipole strength distribution of ^{68}Ni

mean field calculation

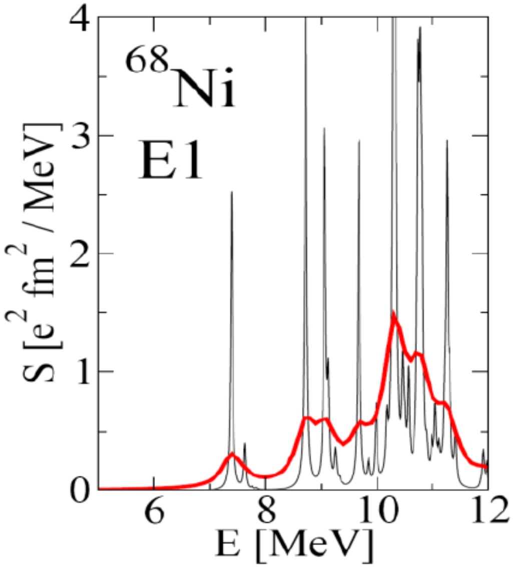

E.Litvinova et al.; PRC 79, (2009) 054312

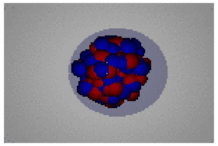

Pygmy resonance

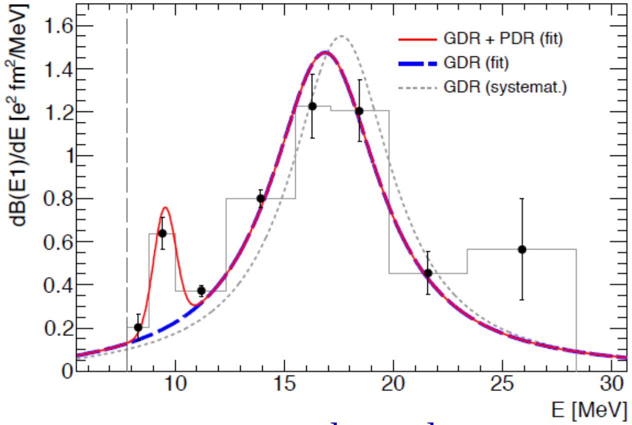

neutron decay data

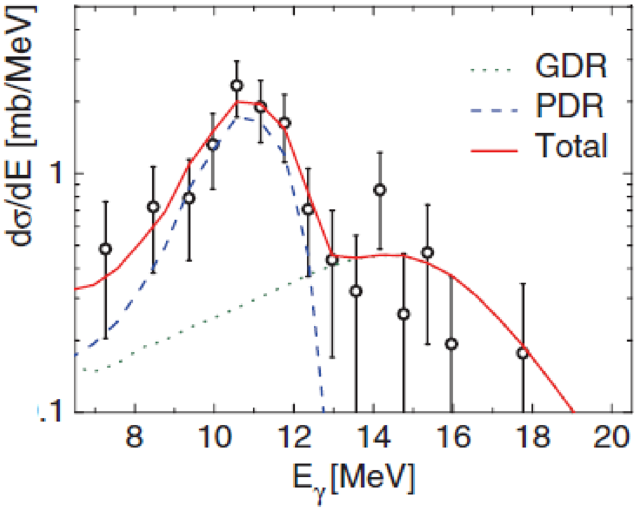

γ-ray decay data

direct γ-decay branching ratio:

Γ_0/Γ = 7(2)%

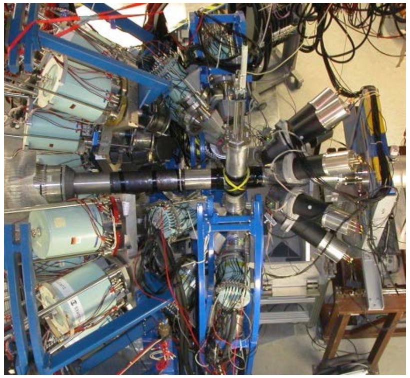

O. Wieland et al.; Phys. Rev. Lett 102, 092502 (2009)

D. Rossi et al.; Phys. Rev. Lett 111, 242503 (2013)